Atmos. Chem. Phys. Discuss., 10, 30473–30537, 2010
www.atmos-chem-phys-discuss.net/10/30473/2010/
doi:10.5194/acpd-10-30473-2010

Atmospheric Chemistry and Physics Discussions

High-ozone layers in the middle and upper troposphere above Central Europe: potential import from the stratosphere along the subtropical jet stream

T. Trickl[1], N. Bärtsch-Ritter[2], H. Eisele[1], M. Furger[2], R. Mücke[1], M. Sprenger[3], and A. Stohl[4,*]

[1]Karlsruher Institut für Technologie, Institut für Meteorologie und Klimaforschung (IMK-IFU), Kreuzeckbahnstr. 19, 82467 Garmisch-Partenkirchen, Germany
[2]Paul Scherrer Institut, Labor für Atmosphärenchemie, 5232 Villigen PSI, Switzerland
[3]Eidgenössische Technische Hochschule (ETH) Zürich, Institut für Atmosphäre und Klima, Universitätsstr. 16, 8092 Zürich, Switzerland
[4]Lehrstuhl für Ökoklimatologie, Technische Universität München, Am Hochanger 13, 85354 Freising-Weihenstephan, Germany
[*]now at: Norwegian Institute for Air Research, P.O. Box 100, Instituttveien 18, 2027 Kjeller, Norway

Received: 28 July 2010 – Accepted: 28 November 2010 – Published: 15 December 2010

Correspondence to: T. Trickl (thomas.trickl@kit.edu)

Published by Copernicus Publications on behalf of the European Geosciences Union.

ACPD
10, 30473–30537, 2010

Abstract

Specific very dry high-ozone layers have been repeatedly observed in the middle and upper troposphere with the ozone lidar in Garmisch-Partenkirchen (Germany), starting roughly two days after the onset of high-pressure periods during the warm season. These episodes, previously not understood, were recently analysed based on extended simulations with the FLEXPART particle dispersion model and jet-stream analyses with the LAGRANTO transport model. The model results indicate import from the stratosphere along the subtropical jet stream over the Pacific Ocean and all the way back to the Atlantic Ocean, in some cases mixed with stratospheric air from intrusions over the North-West Pacific Ocean. Occasionally, also air from the boundary layers of East Asia and North America was admixed. The analysis suggests that stratospheric influence is the most important factor for the increase in ozone and is related to a rather shallow transfer of air from the stratosphere into the rapid upper-and mid-tropospheric air streams observed with the lidar. The in part considerable vertical and temporal extent of these layers and peak ozone mixing ratios between 80 and 150 ppb suggest this to be an important mechanism for stratosphere-to-troposphere transport.

1 Introduction

In all six ozone lidar measurements series covering at least four days, carried out in Garmisch-Partenkirchen (Germany) during high pressure periods between 1996 and 2001 (May to August), we consistently detected very dry air masses above 4 km with peak ozone mixing ratios of 80 to 150 ppb. These specific high-ozone phases typically started two days after the beginning of the respective high-pressure period and, in part, lasted for several days. which indicates an important contribution to the free-tropospheric ozone budget. These observations were not understood at all since they could be neither interpreted by high ozone from North America nor by stratospheric air subsiding over North America or the Atlantic Ocean (Trickl et al., 2003). Two of these

ACPD
10, 30473–30537, 2010

layers contained aerosols indicating the presence of some air from a remote planetary boundary layer (PBL), most likely admixed to these ozone-rich air streams in the vicinity of frontal systems.

Observations of similar very dry air streams were, e.g., reported on by Prados et al. (1999), Bithell et al. (2000), Law et al. (2001) (see also Penkett et al., 2004) and were also found by us in vertical profiles extracted from the MOZAIC (Measurements of Ozone by Airbus In-Service Aircraft (Marenco et al., 1998)) data base. In part, elevated CO has been found and upper-tropospheric advection from the Pacific is indicated. Newell et al. (1999), by analysing MOZAIC vertical profiles, found that atmospheric layers are most frequently associated with an increase in ozone and a simultaneous decrease in water vapour. Typical altitudes are 6 km and the average thickness of layers showing this kind of anti-correlation is of the order of 1 km.

The occurrence of high ozone values in the dry layers seen in our results could suggest the presence of a stratospheric component. But, obviously, the mechanism of stratospheric import leading to such high ozone values in such wide layers must differ from the deep intrusions most commonly observed at our observational site (e.g., Reiter et al., 1971; Eisele et al., 1999; Stohl and Trickl, 1999; Trickl et al., 2003, 2010; Zanis et al., 2003). These deep intrusions are mostly confined to rather narrow air tongues with decreasing ozone mixing ratios as the layers approach the ground. The typical ozone mixing ratios measured in stratospheric streamers at the nearby Zugspitze summit (2962 m a.s.l.) range just between 60 and 80 ppb. There is no way to explain the high mid- and upper-tropospheric ozone concentrations in a layer several kilometres thick by an admixture of such a diluted air mass.

Potential source regions are the atmosphere above the Pacific Ocean and East Asia where frequent and pronounced stratospheric air intrusions may occur (Austin and Midgley, 1994; James et al., 2003; Sprenger et al., 2003). Cooper et al. (2005) report on two strong intrusions in 2004 that even reached Hawaii and led to the observation of 81 and 115 ppb ozone at the Mauna Loa Observatory (3400 m a.s.l.), respectively. The second event (10 March 2004) even reached the sea level, 60 ppb were recorded

ACPD
10, 30473–30537, 2010

at Honolulu. This is particularly remarkable since, at least over Europe, stratospheric intrusions rarely proceed to the ground (e.g., Reiter et al., 1987; Davis and Schuepbach, 1994; Elbern et al., 1997; Eisele et al., 1999; Schuepbach et al., 1999).

Cooper et al. (2004b) also describe that air from a dry intrusion may be mixed into the ascending air streams of adjacent warm conveyor belts (WCBs). In their case study they find that roughly half of the stratospheric component of the dry air stream was dispersed into the upwind and downwind WCBs over the Pacific Ocean. The stratospheric air mass was then lifted back to the upper troposphere and lower stratosphere where it passed over North America and the Atlantic at rather constant altitude. Quite differently, trans-Pacific transport may also occur almost entirely in the upper troposphere. Very rapid trans-Pacific transport of radon-rich air (half life 3.8 days) in the upper troposphere was reported on by Kritz et al. (1990). Liang et al. (2007) observed a case in which subsequent trans-Pacific and trans-North-American transport of an ozone-rich air mass took place exclusively at high altitudes. The entire passage from the West Pacific to the North American east coast occurred within about eight days. A significant ozone enhancement in the upper troposphere above mid-latitude North America due to import from the stratosphere was concluded by Cooper et al. (2006).

The almost zonal propagation of air masses to the east at high altitudes described by Cooper et al. (2004a, b) and Liang et al. (2007) exhibits some similarity with what we found for our observations by trajectory analyses. A very intriguing idea for explaining the high ozone values in the dry air streams observed above Garmisch-Partenkirchen would be that of shallow intrusions directly injecting ozone into the jet stream over the Pacific Ocean or further to the west. Sprenger et al. (2003) locate a maximum in occurrence of shallow intrusions (partly exceeding a relative frequency of 30%) between North Africa and the Pacific Ocean between 30° and 40° N. This transfer seems to occur in the vicinity of the subtropical jet stream which is a rather persistent feature along this path.

Although such a stratospheric component would be an attractive solution one must also consider that some of the elevated ozone could be related to air pollution export

ACPD
10, 30473–30537, 2010

from East Asia. The subtropical Western Pacific is one of the two most important inflow regions for WCBs in the Northern Hemisphere (Stohl, 2001). Cooper et al. (2004a, b) emphasize the role of WCBs in transporting Asian air pollution across the Pacific. As mentioned above they found that these air streams may merge with stratospheric air (see also Liang et al., 2007). As the lofted layers enter North America they stay in the middle and upper troposphere and are rapidly transported to the Atlantic.

Coherent bundles of backward trajectories staying in the middle and upper troposphere between the Pacific Ocean and Garmisch-Partenkirchen have been quite frequently observed, also in other investigations. However, these trajectories had never been followed back beyond a few degrees west of North America. In recent years, we analysed the long-range transport pathways leading to these specific dry layers in some more detail, motivated by the idea of a potentially strong stratospheric contribution to tropospheric ozone, which was, indeed, found. Within the German ATMOFAST (Atmospheric Long-range Transport and its Impact on the Trace-gas Concentrations over Central Europe; ATMOFAST, 2005; AFO 2000) project backward model simulations have been extended to fifteen and now even twenty days in order to provide the missing origins of the anomalously high ozone values. In this paper, we summarize the outcome of these investigations. We found strong similarities between the six cases analysed, but also clear differences in the details, in particular in the importance of the Asian and North American contributions. Most importantly, there are strong hints that the vertical exchange along the subtropical jet stream mentioned above is an important supplier of the high ozone concentrations observed with the lidar.

We focus on presenting just three of the six cases, which represent different behaviour: exclusively stratospheric influence (accompanied by a separate layer also containing some North American air, Case 1, Sect. 3.1), a mixed contribution from the stratosphere and the Asian PBL (Case 2, Sect. 3.2), as well as a situation where two layers with both possibilities co-existed (Case 5, Sect. 3.3). The layers with Asian contributions also include air from the North American PBL. More material on the analysis of five of the six case studied has been presented before (Trickl et al., 2009).

ACPD
10, 30473–30537, 2010

The analysis is now extended to localizing the jet-stream positions and visualizing the trans-tropopause transport in their vicinity.

2 Methods

2.1 Measurements

In this study we use data from measurements with two lidar systems at IMK-IFU (47°28′37″ N, 11°3′52″ E, 730 m a.s.l.). The tropospheric ozone lidar (740 m a.s.l.) was completed in its first version in 1990 (Kempfer et al., 1994) and upgraded in 1994 and 1995 (Eisele and Trickl, 1997, 2005). It has a unique vertical range between 0.2 km and roughly 15 km above the ground, features low uncertainties of about ±3 ppb in the lower troposphere and ±6 ppb (under optimum conditions) in the upper troposphere. The upper-tropospheric performance may be degraded in the presence of high lower-tropospheric ozone concentrations absorbing a lot of the ultraviolet laser emission and by enhanced sky light in summer, in particular in the presence of clouds. The vertical resolution is dynamically varied between 50 m and a few hundred metres, depending on the signal-to-noise ratio that decreases with altitude. The lidar has been used in numerous investigations focussing on atmospheric transport (Eisele et al., 1999; Stohl and Trickl, 1999; Seibert et al., 2000; Carnuth et al., 2002; Roelofs et al., 2003; Trickl et al., 2003, 2010; Zanis et al., 2003).

Aerosol backscatter coefficients were taken from the 313-nm channel of the ozone lidar or from measurements with the big aerosol lidar at IMK-IFU (730 m a.s.l.), a primary instrument of the Network of the Detection of Atmospheric Composition Change (NDACC). This system was originally built in 1973, based on a ruby laser, and has been continually used for measurements of stratospheric aerosol since 1976 (e.g., Jäger, 2005; Deshler et al., 2006; Fromm et al., 2008, 2010). The lidar was converted to a spatially scanning system in the early 1990s for additional investigation of contrails (Freudenthaler et al., 1994, 1995) and, for the routine measurements, has been

ACPD
10, 30473–30537, 2010

operated at the wavelength of 532 nm ever since. The measurements discussed here were either routine early-night stratospheric measurements (vertical pointing, range: 2 km a.s.l. to more than 40 km a.s.l.) or campaign measurements (May 1999, at elevation angles mostly of 25 to 45 degrees in order to improve the coverage of the PBL). For an optimum signal-to-noise ratio in the upper troposphere we evaluated only measurements for the highest angles. With this system rather small aerosol structures exceeding roughly 2% of the Rayleigh return at 532 nm (that corresponds to a visual range of more than 400 km above 3 km) can be resolved within the free troposphere. The aerosol backscatter coefficients can be calculated with a relative uncertainty of 10 to 20%.

In addition, in-situ ozone data from the monitoring stations Garmisch-Partenkirchen (745 m a.s.l., at IMK-IFU), Wank (1780 m a.s.l.) and Zugspitze (2962 m a.s.l.) have been used for comparison. These stations are located at distances of about 8 km from the lidar.

In May 1999, a radiosounding system was operated at Krün (47°30′38″ N, 11°16′52″ E, 876 m a.s.l.), 17 km roughly to the east of IMK-IFU, by a team of the Paul-Scherrer Institute (PSI, Switzerland) as a contribution to the VOTALP "Munich" field campaign (VOTALP II, 2000). For the study presented here this system yielded important complementary information for the lidar and station measurements in the Garmisch-Partenkichen area. A VIZ W-9000 LORAN-C radiosonde was used (http://www.sippican.com). Each sounding provided the standard meteorological parameters pressure, temperature, relative humidity, and horizontal wind vector as a function of altitude. Relative humidity was measured with a fast-response carbon hygristor. Ten of the sondes were equipped with an additional ozone sensor, a Model Z ECC O_3 sonde of EN-SCI Corporation, Boulder, Colorado, that uses an electrochemical concentration cell to measure the ozone concentration (Komhyr, 1969). Sonde measurements were performed from 26 to 28 May 1999, with a total of 16 ascents in irregular intervals during daylight hours.

ACPD
10, 30473–30537, 2010

As in the preceding publications (Stohl and Trickl, 1999; Trickl et al., 2003) we use ozone and water-vapour data from the MOZAIC (Measurements of Ozone and Water Vapor by Airbus In-Service Aircraft) project (Marenco et al., 1998) that have been routinely made onboard five commercial airliners, again for the May 1996 case (see below). This dataset provides daily vertical profiles over Europe, transects at cruising altitude over the North Atlantic and occasional vertical profiles at various locations over North America.

2.2 Models

The transport pathways and source regions were identified by calculations with the FLEXTRA trajectory model (Stohl et al., 1995; Stohl and Seibert, 1998) and the FLEXPART particle dispersion model (Stohl et al., 1998, 2005; Stohl and Thomson, 1999). Both models were driven with operational analyses from the European Centre for Medium-Range Weather Forecasts (ECMWF) with $1^{\circ} \times 1^{\circ}$ resolution. Analyses at 00:00, 06:00, 12:00 and 18:00 UTC and 3-h forecasts at intermediate times (03:00, 09:00, 15:00, 21:00 UTC) were used.

In this study, ten-day backward trajectories were taken as the primary tool for visualizing the altitude of confined air streams that stay in the middle and upper troposphere. The advantage of FLEXTRA trajectory calculations is that certain properties (such as position, potential vorticity and potential temperature) can be tracked unambiguously as a function of time. However, trajectory analyses are problematic for the investigation of very long transport pathways due to the neglect of dispersion as a result of turbulence and convection and a decreasing horizontal density (coverage) as one goes backward in time. Therefore, backward calculations with the FLEXPART model as described in previous studies (e.g., Stohl et al., 2003; Trickl et al., 2003; Huntrieser et al., 2005) have become the principal analysis tool.

FLEXPART calculates the trajectories of a multitude of particles using the mean winds interpolated from the meteorological input fields plus random motions representing turbulence. For moist convective transport, the scheme of Emanuel and Živković-

ACPD
10, 30473–30537, 2010

Rothman (1999), as described and tested by Forster et al. (2007), is used. FLEXPART was run either fifteen or twenty days backward in time to produce information on the emission sources potentially contributing to ozone formation in the sampled air masses. Backward simulations are normally released from 250-m boxes stacked vertically, here all the way up to 12 km along the lidar profile, with 40 000 particles released per box.

The primary output of these so-called retroplume calculations is the emission sensitivity, as described by Seibert and Frank (2004) and Stohl et al. (2003), which describes the pathway of the sampled air mass. The value of the emission sensitivity (in units of $s\,kg^{-1}$) in a particular grid cell is proportional to the particle residence time in that cell. It is a measure for the simulated mixing ratio at the receptor that a source of unit strength ($1\,kg\,s^{-1}$) in the respective grid cell would produce. The emission sensitivity in the lowest layer (so-called footprint) can also be folded (i.e., multiplied) with the distribution of the emission flux densities (in units of $kg\,m^{-2}\,s^{-1}$) from a suitable emission inventory to yield a so-called source-contribution map, that is the geographical distribution of sources contributing to the simulated mixing ratio at the receptor. Spatial integration of the source contributions finally gives the simulated mass mixing ratio in the tracked air mass box at the lidar location. By combining simulations for all altitudes, vertical profiles of tracer mixing ratios split into contributions from different continents, can be displayed. The emissions were taken from the EDGAR 3.2 inventory for the year 1995 or 2000 (Olivier and Berdowski, 2001). For some simulations (see below), the regional inventory of Frost et al. (2006) was used for North American emissions. The emission sensitivities are calculated for a passive tracer, i.e., loss processes are not included in the simulations. Thus, source contributions quantify the total emissions that have entered the sampled air mass during the tracking period. For the analyses presented in this paper we mostly select CO and SO_2 as emission tracers, SO_2 being indicative of contributions from China due to the strong coal burning.

In addition to the emission sensitivities, FLEXPART also outputs the fraction of particles in the boundary layer and in the stratosphere. The threshold condition for the stratosphere was chosen as 2 pvu (potential vorticity units) polewards from 30°. The

ACPD
10, 30473–30537, 2010

thermal tropopause was applied in the tropics. This information is used extensively for quantifying the contribution from the stratosphere to observed ozone. Furthermore, particle positions are clustered as described in Stohl et al. (2002) to provide summary information on the altitude and position of the retroplumes as a function of time. In retroplume cluster plots, the positions of the individual clusters are marked by a circle with a radius proportional to the number of particles in the respective cluster. The colour of these circles represents their altitude and a number gives the backward time in days. The centroid of the retroplume is also displayed by a trajectory, but as the plumes get complex backward in time the centroid may not be very representative of the entire plume.

FLEXPART simulations for this study were done over a period of several years and, therefore, not all products were available for all cases presented here, or the model set-up deviated slightly from what is described above. We first carried out fifteen-day simulations (e.g., Jäger et al., 2004; Kanter et al., 2004) to identify the most important long-distance pathways. These simulations comprised a valuable special feature not available in the later analyses: They highlight the areas where an altitude of 12 km was reached or crossed, i.e., where stratosphere-to-troposphere transport (STT) might have occurred at sufficiently high latitudes. These calculations were never repeated with a 2-pvu potential-vorticity threshold because of the end of the subproject. The fifteen-day simulations differ from the later ones also in the particle release just from a single larger time-altitude box. Recently, twenty-day calculations were added in order to harden the findings for fifteen days and to benefit from the full set of analysis products described above. Most importantly, the twenty-day calculations yield the altitude information for the different quantities, such as the stratospheric fractions and the emissions advected from the different continents.

The role of the jet streams and the vertical exchange between the stratosphere and the troposphere (STE) is elucidated with additional calculations with the Lagrangian Analysis Tool (LAGRANTO; Wernli and Davies, 1997a, b). For five of the six cases (those discussed by Trickl et al., 2009), these calculations allow one to assess bet-

ACPD
10, 30473–30537, 2010

ter how the jet streams and STT in their vicinity influence the observations over Garmisch-Partenkirchen. The calculations are based on the ERA-40 re-analysis data set of ECMWF forecasts in the entire Northern Hemisphere and identify STT and TST (troposphereto-stratosphere transport) according to the methods presented by Wernli and Bourqui (2002), Sprenger et al. (2003) and Sprenger and Wernli (2003). Roughly 7×10^5 trajectory parcels per day were released in the troposphere and stratosphere, each representing a box of initially 80 km×80 km×30 mbar. Whenever a trajectory crosses the 2-pvu tropopause the latitude, longitude, time and pressure at the crossing are saved. Furthermore, transient crossings are excluded by invoking a residence time criterion: the trajectories must be within the stratosphere for 48 h prior and within the troposphere 48 h after the crossing for STT, and vice versa for TST. In the figures, the wind speed is shown at 200 mbar and all STT and TST events within a vertical range from 250 to 150 mbar are marked.

3 Results

All six cases mentioned in the introduction were analysed in detail. An overview is given in Table 1. As further explained in Sect. 3.1 the lidar observations were made under rather similar meteorological conditions, i.e., starting with the clearing at the end of a trough period and extending several days into a high-pressure period. A rather similar principal layer structure has been found during the first two days, related to the impact of three different kinds of long-range transport (Trickl et al., 2003; see Sects. 3.1 and 3.3). After roughly two days consistently additional mid- and upper-tropospheric high-ozone import from beyond America was registered, which is the topic of this paper.

We focus here just on some aspects of three selected cases (1, 2 and 5). More information, also on Cases 3 and 6, was given by Trickl et al. (2009). For Case 4 only a single full-size FLEXPART twenty-day backward analysis was made (23 June, 22:00 CET (Central European Time (CET) = UTC + 1 h)). This model run confirmed the principal transport pattern found for the other cases. Additional trajectory calculations

ACPD
10, 30473–30537, 2010

ensure that the air masses arrived from the Pacific Ocean for the entire period specified in Table 1.

Figures with the colour-coded lidar time series have been presented before for Cases 1 to 4 and 6 (e.g., Eisele et al., 1999; Trickl et al., 2003; Trickl et al., 2010). Therefore, they are not included here again. The only series shown is that for Case 5 (Sect. 3.3).

3.1 Case 1: 31 May 1996

3.1.1 Background

The measurements with the ozone lidar in Garmisch-Partenkirchen during a short high-pressure period between 29 May and 1 June 1996, have been intensively discussed previously. They were carried out to study a predicted stratospheric air intrusion (Eisele et al., 1999) and have been the subject of several modelling efforts including model validation and intercomparison (Feldmann et al., 1999; Stohl et al., 2000; Cristofanelli, 2003; Meloen et al., 2003). This time series yielded the first evidence of significant trans-Atlantic transport of ozone (Stohl and Trickl, 1999 (remark in Sect. 5); Trickl et al., 2003).

The temporal development of the vertical distribution of ozone is, at most altitudes, related to an anti-cyclonic advection pathway around the northern part of a high-pressure zone during its early phase, and a somewhat straighter arrival from westerly directions at some altitudes when the high-pressure zone moves further to the east (Trickl et al., 2003). The arrival path of the deep stratospheric air intrusion observed at the beginning differs since its source region is located between Greenland and Norway (Stohl et al., 2000). As a consequence of three different principal contributing source regions a descending three-layer structure is seen within the free troposphere (see Sect. 3.3 for a similar example), representing an “inverted atmosphere”, with the stratospheric air at the bottom and two layers of PBL air above the intrusion.

The first layer above the intrusion is related to anti-cyclonic low-ozone import from the subtropical Atlantic. High-ozone layers of trans-Atlantic origin were observed above

ACPD
10, 30473–30537, 2010

4 km almost during the entire period. The North American ozone contributions were concentrated mostly above 8 km until the end of the observations and also in a separate layer that gradually descended to 4 km and disappeared during the first hours of 31 May. The most important source regions were Texas, Mexico and, to some extent, also the south-western United States (US). Some uncertainty exists concerning the impact of a large convective cell in the frontal system lifting the air masses to the mid-troposphere. Most importantly, significant stratospheric air inflow into the troposphere could be excluded over North America and the Atlantic.

3.1.2 Observations

The layer of interest in this study overpassed Garmisch-Partenkirchen on 31 May above 5 km. It could not be analysed in our 2003 study due to the insufficient model domain covering just North America and the Atlantic. These model simulations showed some ongoing North American influence in the upper troposphere (see above), but, on 31 May, they did not yield any evidence of a significant PBL contribution in a high-ozone layer between 5 and 7 km (towards the end: 5 to 8 km) during a major part of this day. An example of an ozone profile from this period, measured at 19:00 CET, is shown in Fig. 1 together with a MOZAIC ozone and a humidity profile for Frankfurt several hours earlier (same MOZAIC profiles as in the preceding publication). These two measurements show the best mutual agreement on that afternoon, which reflects the fact that Garmisch-Partenkirchen was approximately downwind of Frankfurt (distance: roughly 330 km) and the ascent route of the MOZAIC Airbus towards the Netherlands. The air mass was very dry indicating that a potential stratospheric air admixture from beyond North America could have created the high ozone values. The considerable width of the layer suggested a potentially strong contribution to STT and, thus, motivated an extension of the analysis. In addition, the presence of a polluted Asian air mass was considered.

The backscatter profiles for 313 nm ("off" wavelength of the ozone lidar) reveal the presence of aerosol between 8 and 9.5 km in the measurements on 31 May, indicating

ACPD
10, 30473–30537, 2010

long-range advection from a remote PBL. This structure just slighty exceeds the strong background noise from Rayleigh backscattering at 313 nm. The example with the least noisy base line close to the 19:00-CET ozone measurement is included in Fig. 1. The maximum particle backscatter coefficient β_P in that layer (8.6 km) corresponds to just 7% of the Rayleigh backscatter coefficient, which, nevertheless, means a significant contribution. The NDACC measurement with the big aerosol lidar on 31 May was made at about 21:30 CET, i.e., at the end of the period with the highest ozone values (not shown). There was, still, minor aerosol around 8 km, discernible due to the much lower Rayleigh background at 532 nm. During the entire period of interest on 31 May no aerosol is seen in the region between 4 km and that aerosol peak next to 8 km, in agreement with our earlier conclusion of an absence of a North American component in the region around the 95-ppb ozone hump in Fig. 1.

3.1.3 Retroplume analysis (FLEXPART)

In order to identify the origin of the elevated ozone concentrations on 31 May fifteen-day FLEXPART backward ("retroplume") simulations were carried out for the two altitude ranges of interest above Garmisch-Partenkirchen (5 to 7 km and 7 to 10 km a.s.l.) and a major part of that day (see Figs. 2 and 3). The emission sensitivities are shown for the PBL (in the third panel also folded with NO_x emissions to highlight the source regions) and 12 000 m, as well as integrated over the entire column. 12 000 m was selected in order to show that an extension of the upper-tropospheric air flow to the west exists as well as for providing a crude guess of the locations of potential transitions from the stratosphere into the troposphere.

The simulation for the altitude range between 5 and 7 km (Fig. 2) confirms the absence of a significant PBL contribution in this layer. This supports the idea of stratospheric influence on the observed ozone rise. In agreement with our earlier findings no significant stratospheric influence is seen over North America and the Atlantic (Trickl et al., 2003). This could be quite different over the Pacific. The 12 000-m panels of both Figs. 2 and 3 show clear sensitivity signatures over the West Pacific between roughly

ACPD
10, 30473–30537, 2010

30° and 60° N. Some of the high-altitude air mass travels backward even once around the globe within fifteen days (Fig. 3) following a route overlapping with the streak of maximum "shallow-fold" activity published by Sprenger et al. (2003).

12 km does not necessarily represent the tropopause at low latitudes. However, a rather big intrusion is indicated in Fig. 3 between Kamchatka and about 40° N, 180° E. The existence of this intrusion was verified also by forward trajectory calculations initiated over that area. It was found that the trajectories mostly stay above 5 km and proceed towards North America and, in part, Europe.

The interpretation did not change when we recently extended the FLEXPART simulations to twenty days. These simulations yielded average altitudes of the backward plume, average fractions of STT for all twenty days and more certainty about a potential overlap with the PBL of East Asia. The vertical profile of the STT fractions for the (most important) earliest days, obtained for the measurement in Fig. 1, is shown in Fig. 4. For 19:00 CET, there is some obvious positive correlation with the ozone structure in Fig. 1, even including the smaller peak at 4.5 km. Figure 5 gives some more details of the analysis for three different altitude bins with different STT fractions, representing the respective layers. The second panel of Fig. 5 shows the result for the bin (5500 to 5750 m) with the highest stratospheric influence in that layer (Fig. 4), found on days −20 to −15. For the early period the fractions do not vary much, a rather general behaviour for all cases (even over more days, see Sect. 3.2). The vertical distribution of the mean cluster positions shows one component staying at 10 km and higher for an extended period of time, in contrast to the other two panels corresponding to layers with almost negligible STT. This behaviour supports the idea of shallow STT.

12% of stratospheric influence looks moderate, but can be converted into an ozone enhancement by up to 60 ppb, assuming ozone values of up to 0.5 ppm within the first few kilometres above the tropopause as seen in many lidar measurements. It is interesting to note that, at this late time (19:00 CET), there is little influence from the intrusion over Kamchatka, suggesting that, in this example, most of the STT takes place along the long lower-latitude branch of the backward plume.

ACPD
10, 30473–30537, 2010

In the upper troposphere (Fig. 3 and lowest panel in Fig. 5) PBL contributions coexisted with stratospheric contributions, except for a short gap with low STT fractions around 8.9 km. The air flow in this altitude range was much faster, with transport times between the Pacific and Garmisch-Partenkirchen of less than ten days, as already revealed by our earlier trajectory analysis (Trickl et al., 2003). Pronounced contributions from various polluted regions around the Gulf of Mexico, Mexico City and from Southern California are seen. The local air-quality station network in Mexico City reports peak values between 180 and almost 230 ppb between 12 and 18 May, 125 ppb on 19 May, and between 150 and almost 270 ppb until the end of May (http://www.sma.df.gob.mx/simat/home_base.php). Again, Asian contributions are almost absent. This can also be seen from the calculated vertical distribution of the emissions from the different continents reaching Garmisch-Partenkirchen shown in Fig. 6. The maximum PBL contribution is located between 8 and 9 km, exactly where the aerosol peak was found with both lidar systems.

3.1.4 Jet-stream and Lagrangian STE analysis (LAGRANTO)

Motivated by FLEXPART results in the "12 000-m" panels of Figs. 2 and 3 (also in the cases discussed in the following sections) and the results by Sprenger et al. (2003) the idea of STT along the subtropical jet stream as a potentially important source of the elevated ozone in our observations was born. Recently, additional visualizations of the jet streams in the Northern Hemisphere were derived from the ERA-40 re-analysis, starting about fifteen days before the beginning of the respective high-ozone period. The results were plotted at intervals of six hours. In Fig. 7 we show images for four different times, corresponding to an eastward propagation of the air parcels.

The subtropical jet stream exhibits changes in wind speed, but no strong latitudinal variations as the sub-polar jet. It can, thus, can be compared relatively well with the position of the "12000-m" section of the FLEXPART backward plume. The agreement is excellent. The jet stream follows the FLEXPART plume to North America, with an obvious northward motion over the Pacific and North America. All along the jet verti-

ACPD
10, 30473–30537, 2010

cal exchange between the stratosphere and the troposphere takes place, confirming the conclusions for the FLEXPART calculations. In particular, the STT dots are found exactly where they would be expected from Fig. 3, e.g., next to the Strait of Gibraltar in the top panel and further to the east (Caucasus, China, south of Japan) in the following ones. The downward transport marked by the green dots seems to occur preferentially on the north side of the subtropical jet stream, as one would expect from the counter-clockwise rotation of the air-masses around the jet (see Sect. 4). It is interesting to note that sometimes STT and TST (troposphere-to-stratosphere transport) simultaneously occur in the same confined area, which is in some agreement with the idea of shallow exchange. A clear assignment of the locations of STT or TST to the phase of a single high-velocity streak is not easily possible. On the day of arrival over Garmisch-Partenkirchen the jet stream is located north of Germany (not shown). Thus, the high-ozone air mass does not approach the observational site inside the jet stream itself as initially thought. However, due to the rather short transport time once around the globe most of the transport must take place not too far away from the locations of the highest velocities.

3.2 Case 2: May 1999

3.2.1 Background

The ozone series between 26 and 30 May 1999, showed the longest persisting high mixing ratios ever observed with the ozone lidar in the middle and upper troposphere above Garmisch-Partenkirchen (Trickl et al., 2003). The ozone mixing ratio above 4 km reached values between 80 and roughly 150 ppb. The analysis showed sources in the North American PBL, but also a strong, almost horizontal high-altitude flow from the Pacific to Europe. On 27 May, 70 to 80 ppb were observed also below 4 km and ascribed to direct input from the Eastern US, one of the rare cases in which this has led to the observation of a pronounced rise in ozone at the Zugspitze summit (see (Stohl et al., 2003) and (Huntrieser et al., 2005) for another example). The NO_y mixing ratios at

ACPD
10, 30473–30537, 2010

the nearby Wank station (1780 m a.s.l.) were just between 1 and 2 ppb which indicates a moderate European contribution to this air mass.

During that period a VOTALP II field campaign took place, devoted to the investigation of the transport of the Munich plume into the Alps, in particular in the Loisach and Isar valleys (VOTALP II, 2000). The mobile radio-sounding station, operated by the PSI team at Krün between 26 and 28 May (see Sect. 2.1), yielded similar ozone profiles as the lidar, the only major difference being vertical displacements due to orographic lifting of the sonde. In addition, frequent measurements with the big aerosol lidar were made during this field campaign, yielding information on potential contributions from remote boundary layers. Due to the availability of all these complementary measurements we discuss this period in particular detail. In the following we present four examples from the period during which all system were operated. We describe here mostly the analysis of 27 May, that of the other days being included in (Trickl et al., 2009).

After a final frontal passage on 23 May a long high-pressure zone formed that extended from the region south of Newfoundland to 30° E on 24 May. A stratospheric intrusion would be expected to occur during the transition to high pressure. However, there is only a slight indication of an intrusion in the Zugspitze ozone and humidity data. We assume that the intrusion was shifted to the east in the rapid eastward air flow north of the Alps.

3.2.2 Observations

Due to the preparations for the field campaign no lidar measurements were made on the first two days of this high-pressure period. The measurements were started in the early afternoon of 26 May, and immediately showed the high-ozone layer that was observed over many days. Figure 8a shows one example of soundings on 26 May at about 16:00 CET, when the first PSI ozone sonde was launched. The principal agreement between lidar and sonde in that obviously spatially rather inhomogeneous ozone plume is not perfect, but acceptable. The lidar data are confirmed up to 3 km by the measurements at the nearby local monitoring stations, whereas the sonde should have

ACPD
10, 30473–30537, 2010

departed more to the east.

Above 4 km elevated ozone is correlated with low humidity and, in part, with aerosol. Both the ozone lidar (affected by a small light leak in the receiver box during that campaign) and the PSI data, unfortunately, end just above 7 km. However, the aerosol lidar detected significant traces of particles between 7.3 km and 11.7 km, the latter value agreeing with the tropopause levels determined by the Munich radiosonde (11.6 km at 12:00 UTC and 11.8 km at 24:00 UTC). A closer look at the trajectories calculated for our earlier study (Trickl et al., 2003) suggests that at least some of this aerosol could be associated with an ascending air stream from the mid-west of the US. There, 60 to 80 ppb of ozone were observed, too low for explaining the values at the upper end of the sounding range. However, there is also a thick, almost horizontal trajectory bundle above 5 km leading backward to the west coast of North America suggesting potential additional sources of ozone beyond North America, as for Case 1.

Figure 8b and c show very high ozone and aerosol values on 27 May 1999, correlated with low relative humidities down to 5% (please, note in Fig. 8c the vertical offset of the lidar and the sonde data above 3.3 km). The aerosol peaks for the 532-nm measurements reach almost $10^{-5}\,(\mathrm{m\,sr})^{-1}$, which is rather remarkable for the free troposphere and corresponds to a visual range of less than 10 km. Such values are almost one order of magnitude higher than typical values for aerosol structures related to intercontinental transport, even in fire plumes from the US observed during strong fire years (see Sect. 4). The analysis by Trickl et al. (2003) showed mixed input from different parts of the US into a rather horizontal air stream, but, again, a number of middle and upper-tropospheric trajectories indicate a contribution to the high-ozone air mass from beyond North America.

The fourth example (Fig. 8d) is from a period on 28 May (not analysed in our earlier publication) between an early-morning thunderstorm and rain in the afternoon. There was much less aerosol, but, still, the ozone values were high and the corresponding humidity was low. Before the thunderstorm the ozone values had reached almost 150 ppb (03:00 CET). There is not much indication of a PBL contact over North America within

ACPD
10, 30473–30537, 2010

the ten days of trajectory calculation time. Most trajectories end over the subtropical Atlantic to the north-east or east of Cuba, at altitudes between roughly 3 and 9 km. Those in the uppermost troposphere, again, extend from this area further to the west and reach the Pacific.

3.2.3 Retroplume analysis (FLEXPART)

As mentioned we mostly concentrate on describing the analysis for 27 May, but we include also a few remarks concerning the other two days.

As a first step for extending the analysis with respect to that by Trickl et al. (2003), a fifteen-day FLEXPART backward simulation was carried out for the high-ozone layer between 5 and 9 km on 27 May (Fig. 9). The result for 12 000 m looks similar to that in Fig. 3. It, again, indicates a possibly strong contribution from a stratospheric intrusion over the Northern Pacific and reproduces the second branch reaching back to the Mediterranean Sea. However, in this case some Asian air pollution was admixed to the air stream. It is interesting to note that the backward simulations show significant contributions from several source regions in the entire US not identified by the 10-d backward trajectories studied by Trickl et al. (2003), in particular California, which demonstrates the better coverage of remote areas by the retroplume results.

As for Case 1 the simulations were more recently extended to twenty days for all the times of the examples in Figs. 8a to 8d in order to harden the stratospheric influence and to obtain a better estimate of the role of the Asian emissions based on the potentially better overlap with the countries in the Far East.

In Fig. 10 we give an overview of the vertical distributions of the stratospheric fractions calculated for the four measurements shown in Fig. 8. Again, the highest STT fractions extracted from the FLEXPART calculations are reached within the earliest days. We, thus, limit the values to those for days −20 to −15. Clearly, the maximum stratospheric fractions for all four measurements discussed are higher than those for Case 1, in qualitative agreement with the, in part, much higher observed ozone concentrations. A comparison of the two profiles for 27 May (Fig. 10b) with the measured

ACPD
10, 30473–30537, 2010

ozone and aerosol profiles, despite nicely reproducing the main features, indicates some noise component in the numerical results: There is less difference between the two measurements than between the two simulated fraction profiles. Despite the fine structure seen in the experimental and modelled results in the range between 5.5 km and 9 km the transport pathway does not change much. Differences are only seen over Asia, as indicated by the broadening of the plume section for 12 km in Fig. 10.

In Fig. 11 we give three examples of retroplume summaries for specific layers in Figs. 8c and 10b, one below the range with elevated stratospheric fractions, two within this range. In particular, in the range of the strongest peak in the aerosol profiles the FLEXPART stratospheric fraction is the highest, and elevated fractions extend over more than 17 days. The FLEXPART particle clusters in the upper boxes of the two lower panels do not suggest the presence of a component from deep STT. In contrast to the simulation presented in Fig. 9 some pick-up of stratospheric air over Canada and the north-western Atlantic was found, which corresponds to the peak in the third panel of Fig. 11 at −4 d.

Also import from the East Asian PBL is seen. From the emission sensitivity "footprints" it is obvious that PBL contact over East Asia peaks for air masses arriving over Garmisch-Partenkirchen in the range between 7.25 km and 8 km, i.e., in the altitude range of the big aerosol peak in Figs. 8b and 8c. This is confirmed by the vertical distribution of the emissions transported to Garmisch-Partenkirchen, (Fig. 12; see in particular SO_2). Also some overlap of the backward plume with the desert regions is found. The aerosol images from the Total Ozone Mapping Spectrometer (TOMS, http://toms.gsfc.nasa.gov/aerosols/aerosols.html) reveal pronounced dust outbreaks in the Takla Makan and Gobi deserts during the entire month of May. It is, thus, likely that at least the big aerosol peak in Figs. 8b and 8c between 7 and 8 km is caused by dust from the Asian deserts. The satellite images do not show any other significant source of aerosol in sufficient vicinity to the FLEXPART plume.

The FLEXPART results suggest even stronger Asian influence for 26 May (Fig. 13) although the aerosol contribution is lower here (Fig. 8a). This indicates less influence

ACPD
10, 30473–30537, 2010

from the deserts and more pick up of air pollution from the East Asian PBL. The Asian influence seems to be higher in the altitude range with the highest aerosol backscatter coefficients (5.5 km to 6.5 km) whereas in the lower-aerosol range between 7.2 km and 11.9 km a stronger North American fraction seems to exist (see subsection on observations). On 28 May (Fig. 8d) the influence of the continental boundary layers seems to be low. Here, very likely, the stratospheric influence dominates.

In summary, we conclude also for the high-ozone layer observed in this case study the presence a highly significant stratospheric component, however, mixed with PBL air during certain periods. The transport pattern resembles that in Case 1.

3.2.4 Jet-stream and Lagrangian STE analysis (LAGRANTO)

Also for Case 2 an attempt was made to relate the long part of the FLEXPART backward plume, which reached back to the Mediterranean Sea, to vertical exchange (STT) along the subtropical jet stream. Four examples are given in Fig. 14. Again, a good general agreement of the plume component in the 12-km panel of Fig. 9 is found. However, over a major part of Asia less STT events are marked than in the images for Case 1. This could, in part, be due to the rather restrictive selection criterion (see Sect. 2.2). Also the potential vorticity threshold of 2 pvu might be too high for the subtropics (Folkins and Appenzeller, 1996; Gouget et al., 1996).

3.3 Case 5: 21 to 24 July 2001

3.3.1 Observations

The lidar measurements between 21 and 24 July (Fig. 15) yielded a particularly nice example of the May-1996 type (Case 1), in an analogous way related to a high-pressure zone moving into Central Europe. An ozone layering typical of this kind of weather situation is seen, with stratospheric air (S) descending towards the PBL in the early phase, low-O_3 air from the subtropics above this layer (SA) and air from beyond the

ACPD
10, 30473–30537, 2010

Atlantic above 4 km (see Sect. 3.1).

The temporal development above 4 km starts with the arrival of PBL contributions from the US. The principal source region was first the north-eastern part of the US, later there was also input from other regions. Again with a delay of about two days there was a conspicuous ozone increase between 6 and 8 km, here to values of about 120 ppb. The correctness of the measurements was verified by a comparison with the Hohenpeißenberg ozone sonde on 23 July 2001, launched at 05:41 CET (difference at the ozone peak at 7.5 km: +7 ppb for the lidar). From the ozone structure we distinguish several layers. The analysis focusses on the three layers labelled in Fig. 15 as L1 to L3.

Since low humidity had been found in the analogous cases we analysed the MOZAIC data for Frankfurt and radiosonde data from the surrounding stations Payerne, Stuttgart and Munich (not shown). The situation is rather complicated due to the strongly altitude- and time-dependent wind direction (see Figs. 16 and 17). For the layer around label L1 Payerne is the most adequate station due to westerly advection and, indeed, shows relative humidities of 20% and less between 5 and 7.5 km. For the higher altitudes Stuttgart (north west) is the better choice during the early phase due to north-westerly advection, with relative humidities between 10 and 20% in the entire troposphere above 5.6 km. However, also close to the L3 period relative humidities of down to 11% are seen above 8 km, presumably because of an advection parallel to that above Garmisch-Partenkirchen.

3.3.2 Vertical Positions of the air streams (FLEXTRA trajectories)

Because of the spatial confinement of the most relevant air masses a particularly clear picture of the three-dimensional transport path from 140° W to Garmisch-Partenkirchen is obtained from ten-day FLEXTRA trajectory plots. Two examples for the period of the layers L1 to L3 are shown in Figs. 16 and 17. An onset of air-mass import from the Pacific is observed in the afternoon of 22 July, for altitudes above the lidar between 6 and 8 km a.s.l. The advection pathway covers parts of Canada and the Northern

ACPD
10, 30473–30537, 2010

US. For the 01:00-CET calculation (Fig. 15) the upper-tropospheric trajectories (layer L2) mostly correspond to air masses ascending from the PBL over North America and the western part of the Atlantic. The trajectories for layer L1 stay in the upper troposphere and even slightly ascend backward in time as they approach the Pacific. The situation changes in the afternoon of 23 July, when most trajectories above 5 km stay at high altitudes and end over the Pacific (Fig. 16). There is some indication of separate trajectory bundles for layers L1 and L3. The potential vorticity south of Alaska is less than 1 pvu suggesting the absence of a local intrusion in this area.

3.3.3 Retroplume analysis (FLEXPART)

Fifteen-day backward simulations with FLEXPART were carried out for all the three layers. We only show the results for layer L3 (Fig. 18). The simulations for the other two layers look similar, but without a clear contact with the East Asian PBL within fifteen days. In addition, for L1 a pronounced intersection of the particle plume with 12 km is seen over the Atlantic between 157° and 45° N that is missing in the case of L2 and L3.

The results in Fig. 18 for 12 000 m altitude, again, indicate potential STT over the Pacific. As in the first two cases, intersections with this level are seen all the way back between the Pacific and the East Atlantic (more than once around the globe). The particle band for for 12 000 m starts exactly in the region where the trajectories in Fig. 17 leave the panel. It follows the column sensitivity even over Asia, suggesting a single, almost coherent air stream all around the globe, again following the maximum of shallow STT displayed by Sprenger et al. (2003). Moderate PBL contributions from both North America and East Asia are seen.

For three times on 23 July corresponding to L1–L3, 04:00 CET, 07:00 CET and 22:00 CET, twenty-day simulations were performed, which yielded both a better estimate of the potential Asian influence and information on the approximate vertical position of the plume. Not all results are discussed here. The simulations for the earlier two times show elevated PBL contributions above 7 km, increasing towards layer L2 and dominated by North American emissions. Quite obviously, the vertical distribution

ACPD
10, 30473–30537, 2010

of advected emissions does not explain why there is so much more ozone in layer L1 than in layer L2. However, in L1 an elevated single-day stratospheric influence of up to 12% is seen in the FLEXPART results. By contrast, for L2 rather low stratospheric fractions are obtained for the preceding twenty days.

In the case of layer L3, where the highest ozone concentration is found, the stratospheric contribution clearly dominates. Figure 19 shows a vertical distribution of the maximum single-day FLEXPART stratospheric fractions for the backward time intervals five to ten and ten to twenty days as extracted from the retroplume analysis for 22:00 CET. These time intervals cover most of the relevant stratospheric input. The rather pronounced stratospheric peaks correlate well with the observed ozone maxima for 22:00 CET on 23 July. The stratospheric fraction for layer L3 (9 km) is particularly high (63 and 75%, respectively, for the two backward time periods chosen). Given this high fraction, the observed peak ozone mixing ratios of about 120 ppb look somewhat low remembering the findings for the other cases for which lower stratospheric fractions were found. Also a high-resolution hemispheric Eulerian simulation by our project partner EURAD (not shown; for details on the model see (ATMOFAST, 2005; Trickl et al., 2010)) seems to overestimate significantly the stratospheric component in this layer, with ozone mixing ratios strongly exceeding the measured 120 ppb.

The time-altitude plot for layer L3 (not shown) shows four partial clusters of the plume, the upper three always staying above 6 km and the uppermost one never getting below 10 km. This confirms the tendency seen in the trajectory plot (Fig. 17) and, again, suggests rather shallow STT in an upper-tropospheric air stream almost all the way around the globe (starting at −4d).

The vertical distribution of emissions for layer L3 (Fig. 20) show only half the mixing ratios calculated for L1 and L2. But they include a much higher Asian fraction, as already indicated in the fifteen-day simulations. A moderate North American spike at 8 km is likely to be an extension of layer L1.

ACPD
10, 30473–30537, 2010

3.3.4 Jet-stream and Lagrangian analysis (LAGRANTO)

Examples of the LAGRANTO simulations for Case 4 are shown in Fig. 21. The top panel reveals pronounced STT over Morocco, exactly where the backward tongue in the 12-km panel in Fig. 18 ends. The larger spread of the backward plume over East Asia and the bow south of Alaska seem to be confirmed.

4 Discussion and conclusions

The extended backward analyses presented in this paper have added some significant information on mid- and upper-tropospheric dry high-ozone layers rather consistently observed with the lidar roughly two days after the beginning of high-pressure periods. The high-pressure zones under consideration typically enter Central Europe not extending too far to the north of our observational site in the Northern Alps (roughly 1000 km), thus allowing for anti-cyclonic inflow of North American air masses around their northern edge during the early phase (Stohl and Trickl, 1999; Trickl et al., 2003). As the high-pressure zone proceeds to the east a transition to straighter inflow from the Atlantic occurs at some (in some cases: most) altitudes in the free troposphere (see column-sensitivity panels and Figs. 2, 3, 9 and 18) and the direct advection from beyond North America starts at altitudes typically above 5 km. The North American air typically ascends from the PBL to the middle and upper troposphere by transport in warm-conveyor-belts (Stohl and Trickl, 1999) and the backward air parcels for the free troposphere horizontally almost coincide over a major part of the Atlantic. Over North America branching occurs at moderate altitudes. Considerable complexity is added by further prefrontal upward transport (Trickl et al., 2003).

The ozone-rich mid- and upper-tropospheric air streams remain rather coherent and could be mostly followed from Europe backward to the Eastern Pacific even by trajectories. However, there is a clear gain in information for the long travelling times by using the FLEXPART analysis tools. The vertical distributions for the various output quanti-

ACPD
10, 30473–30537, 2010

ties almost perfectly match the lidar results in their layering. The model-based analysis reveals the presence of stratospheric contributions mostly entering the tropophere over the Pacific, Asia, and even further to the west. For just a few of the high-ozone layers simultaneous air pollution import from East Asia and North America was suggested, which hardens the idea of an important stratospheric influence on the ozone increase in the majority of these layers. Their thickness and length varies considerably from case to case (Table 1). A particularly impressive example is Case 6, for which a simulation with the EURAD chemistry-transport model showed the almost complete absence of extra CO from emissions during the entire duration of the high-ozone layer (Trickl et al., 2009, 2010). The transfer from the stratosphere into the, in part, rapidly traveling air streams is very likely rather shallow on average ("shallow and medium folds" as defined by Sprenger et al., 2003).

The fact that the modelled stratospheric component was almost exclusive in the majority of these layers also suggests that these air streams may be associated with a possibly very important mechanism of STT. The layers, containing 80 to 150 ppb of ozone, are several kilometres thick, can sometimes be observed with the lidar for several days and do not resemble the deep intrusions most commonly observed at the nearby Zugspitze summit for a short period of time (Trickl et al., 2010). The humidity in these layers is low, but not negligible, which indicates a contribution of tropospheric air even in the centre of these sometimes quite thick layers. A tropospheric influence is obvious for the cases with aerosol observations.

Two branches are seen that vary in mutual importance from case to case. From our model analysis we cannot distinguish the branching ratio. The first branch corresponds to inflow from stratospheric intrusions over the Northern Pacific not deeply penetrating the troposphere. Such a contribution was found in two of the six cases. The other branch is formed by air masses travelling around the globe between 30°and 40° N within just fifteen days. The 12-km results in the fifteen-day simulations cannot be seen as a full proof due to the moderate latitudes of that component. However, there is some evidence from the twenty-day analyses (in particular Case 5) and the

ACPD
10, 30473–30537, 2010

LAGRANTO results that significant STT should have occurred also here. In fact, these air streams almost co-incide with the maximum of shallow and medium folds obtained by Sprenger et al. (2003). This latitudinal belt seems to overlap with the northern end of the subtropical jet stream on the north side of the Hadley cell, typically between 10° and 30° N.

The subtropical jet is an almost persistent feature exhibiting a rather moderate wave structure (e.g., Krishnamurti et al., 1961; Koch et al., 2006). The Results in Figs. 7, 14 and 21 confirm this behaviour. Its maximum is reached in winter and spring and it is vertically thin in comparison with the polar jet (Koch et al., 2006). The reported shallow-fold formation seems to be located more on its north side. This is confirmed in our analysis for Case 1, but is less clear for the other cases. This is a consequence of the reported counter-clockwise rotation of that air stream (e.g., Krishnamurti, 1961), in agreement with the findings for the mid-latitude jet (e.g., Danielsen, 1968). The downward transport usually starts in regions of acceleration (entrance region, Keyser and Shapiro, 1986). This can be sometimes seen in the LAGRANTO results presented in Sect. 3, in particular in Fig. 7. But there are also deviations and, as mentioned in Sect. 3.1, regions where upward and downward transport even seems to co-exist. This is not easy to understand and indicates a considerable complexity of these processes. The complexity is enhanced by occasional contact with other jet streams. Due to the selection criteria the STT and TST events marked in Figs. 7, 14, and 21 do not give a full coverage of the trans-tropopause transport (see Sect. 3.2). This includes selecting 2 pvu for the tropopause instead of 1 pvu one and less as discussed by Appenzeller (1996), Gouget et al. (1996) and Cammas et al. (1998).

Sprenger et al. (2003) conclude very high folding frequencies of almost 30% in this area that extends from North Africa to the Pacific (and even around the globe during the cold season), in agreement with the persistence of the subtropical jet stream. The reported lower STT penetration depth might, in part, be due to the lower jet-stream curvature (Keyser and Shapiro, 1986) and to a confinement of the jet to the upper troposphere in this area (Koch et al., 2006). In their case study, Gouget et al. (1996) point

ACPD
10, 30473–30537, 2010

out that the descending stratospheric air tongue was quasi-horizontal and that, in contrast to the deep mid-latitude jet front systems, the subtropical front was concentrated in a shallow layer. Cammas et al. (1998) found as many as 154 high-ozone episodes north of 15° N during MOZAIC flights between Europe and South America between August 1994 and April 1997

The results of the jet-stream climatology derived by Koch et al. (2006) resemble the pathways obtained from the FLEXPART and ERA-40/LAGRANTO analyses for the cases examined in our study. The subtropical jet, on a seasonal average, proceeds northward over the Pacific and North America, ending between Iceland and the United Kingdom. The frequency of jet-stream occurrence along this band, in particular over North Africa, is higher in winter and spring than in summer. Four of our six observations took place in spring (Table 1), i.e., during a period favourable for the formation of such air streams. It will be interesting to see if, with a growing coverage of the cold season with lidar measurements in recent years similar middle- and upper-tropospheric ozone maxima can be identified also in winter. However, the hibernal flow pattern over the North Atlantic looks quite different from the situation in the six cases described here.

A comparison of the FLEXPART and LAGRANTO results for the early times suggests that modelling of air flows around jet streams is rather reliable. However, it is presumably difficult to compare the results on a daily basis because of the temporal spread of the backward plumes with time. Field experiments and forward transport model runs for analysing the vertical exchange across the subtropical tropopause and the long-distance propagation of stratospheric air intruded into the upper troposphere are desirable. Another open question is the deviation of the jet stream positions in the ERA-40 material analysed from the arrival pathway over the North Atlantic and Europe. According to the FLEXPART results the minimum travel time of these air masses once around the globe is of the order of fifteen days, corresponding to an average speed of roughly 30 $m\,s^{-1}$. Therefore, it is reasonable to assume some propagation not too far away from the centre of the subtropical jet stream as indicated by the comparison of the model results. Finally, the main open question remains that about the reproducibil-

ACPD
10, 30473–30537, 2010

ity of a pattern in the observations that is related to such an extremely long transport path. This question also addresses the behaviour of the northward spiralling of the subtropical jet stream.

The existence of aerosol in some of the layers indicates contributions from a remote PBL. In the most spectacular case (May 1999) the FLEXPART analysis suggests the presence of dust from the Takla Makan and Gobi deserts. However, it is difficult to quantify the impact of East Asian emissions. There are large uncertainties in the emission inventories (Ma and van Aardenne, 2004). This uncertainty is enhanced due to the strong positive trend in emissions in that region, with more than a doubling of the NO_2 peak values from 1995 to 2004 (Richter et al., 2005; see also Ding et al., 2008). It would be helpful to obtain more observations with dominating East Asian influence. However, such cases are obviously difficult to find and we know of just two studies of Asian plumes reaching Europe after transport across the North Pacific, North America and the North Atlantic (Grousset et al., 2003; Stohl et al., 2007). The analysis of our measurements shows that most of these air streams contain some fraction of North American air pollution. However, a few aerosol observations in the free troposphere in our long-term series (Jäger, 2005) could be traced back to the Pacific area using FLEXTRA results (ATMOFAST, 2005; Jäger et al., 2006) and will be analysed further.

We found by trajectory analyses of free-tropospheric lidar measurements for several years that aerosol is a suitable indicator of PBL air, although its free-tropospheric abundance is mostly low (ATMOFAST, 2005; Jäger et al., 2006). This is perhaps due to washout in the WCBs during convectively lifting the PBL air to the free troposphere, or due to dilution in diverging air masses. In our free-tropospheric soundings available since 1992 the aerosol backscatter coefficients above 3 km have rarely exceeded the Rayleigh background at 532 nm (which corresponds to a visual range of 300 km at sea level) by more than 50%, even during strong fire years in the US. Due to the high sensitivity of our NDACC lidar system (free-tropospheric threshold for aerosols: about 2% of the Rayleigh background) these structures are, nevertheless, clearly visible. Really strong aerosol signatures have only been detected above Garmisch-Partenkirchen

ACPD
10, 30473–30537, 2010

during Saharan dust outbreaks, which typically reach up to 6 km (Jäger et al., 1988; Kreipl et al., 2001; Papayannis et al., 2008), and in boreal fire plumes, e.g., in August 1998 (Forster et al., 2001) and in July 2004 (during the ICARTT (Fehsenfeld et al., 2006) campaign (ATMOFAST, 2005)).

The model results (including the EURAD results not shown here) also reveal that there may be problems in quantitatively predicting the amount of ozone imported from the stratosphere into these rapid air streams. One possible reason could be the pronounced spatial and seasonal variation of ozone in the lowermost stratosphere ranging between 100 and 500 ppb (Thouret et al., 2006). This is confirmed by our lidar measurements that occasionally show strong concentration changes above the tropopause within one to two hours.

The analysis may be further complicated by lightning. In all cases discussed by Trickl et al. (2003), which are also part of the present study, thunderstorms or large convective cells have been detected in areas where PBL air is lifted to the middle troposphere. Huntrieser et al. (2007) conclude from measurements over South America that the outflow from mesoscale convective systems may yield significantly enhanced ozone mixing ratios (roughly from 35–40 ppb to 60–80 ppb in the case described) at distances of several hundred kilometres away from the source. A number of recent publications verify a significant ozone contribution from lightning-generated NO_x for the US and adjacents marine regions (Beirle et al., 2006; Cooper et al., 2006; Liang et al., 2007; Schumann and Huntrieser, 2007; Singh et al., 2007; Sioris et al., 2007). Cooper et al. (2006) conclude from the large data set collected during the ICARTT campaign that most of the ozone enhancement over the Eastern US (excluding stratospheric contributions) in July and August 2004 was due to lightning-generated NO_x.

In many cases mixing of different contributions within or in the vicinity of frontal systems over the Pacific takes place. The proximity of one of the most important WCB inflow region to East Asia is an important factor (Stohl, 2001, and references therein). The WCB lifts the Asian air masses towards the North Pacific where many of the air flows observed above our site pass by. We have started to speculate on a potential

ACPD
10, 30473–30537, 2010

impact of the rising Asian air pollution on the ozone concentrations in the upper troposphere and the lower stratosphere (UTLS). Indeed, an analysis of MOZAIC data between 1994 and 2003 has revealed a positive ozone trend in the UTLS (Thouret al al., 2006). This is confirmed by the analysis of the Hohenpeißenberg sounding record from 1966 to 2007 (Claude et al., 2008), showing a +7.5-%/decade trend after 1994 that is limited to a narrow range around 14 km. A preliminary analysis of the Zugspitze CO within ATMOFAST has yielded a slightly positive trend of CO in stratospheric intrusions since the beginning of the CO measurements in 1990, opposing the slightly negative trend for non-stratospheric conditions (ATMOFAST, 2005).

More measurements are needed to harden further the reproducibility of these observations. In particular, we plan to intensify simultaneous lidar sounding of ozone, water vapour and aerosols. Accurate side-by-side H_2O measurements are needed as an important information for quantifying the tropospheric influence in these dry air streams. Our new high-power water-vapour lidar has yielded humidity profiles for the entire troposphere with just minor restrictions during daytime, as a result of an application of the differential-absorption technique (Vogelmann and Trickl, 2008).

Acknowledgements. The authors thank P. Fabian and W. Seiler for their interest and support. They are indebted to P. James who carried out the 15-day simulations with FLEXPART, but cannot co-author this paper for specific reasons. They thank H. Feldmann for generating plots from the one-year EURAD run for 2001, J. Keller for preparing the PSI sonde system and carefully archiving the data, H. E. Scheel for providing the local station data and H. Claude for making available data from the Hohenpeißenberg sonde archive. Furthermore, they thank the MOZAIC team for allowing them to access their data base, O. Cooper and A. Volz-Thomas for their help with literature, as well as R. Steinbrecher and L. G. Ruiz Suárez for providing the link to the station data for Mexico City. This work has been funded by the European Union within the VOTALP (Vertical Ozone Transport in the Alps, parts 1 and 2), STACCATO (Influence of Stratosphere-Troposphere Exchange in a Changing Climate on Atmospheric Transport and Oxidation Capacity) and EARLINET (European Aerosol Research Lidar Network) projects as well as by the German Bundesministerium für Bildung und Forschung within the programme

ACPD
10, 30473–30537, 2010

"Atmosphärenforschung 2000" (ATMOFAST project: Atmospheric Long-range Transport and its Impact on the Trace-gas Composition in the Free Troposphere over Central Europe) and the German Aerosol Lidar Network.

References

AFO 2000: Results of the German Atmospheric Research Programme, edited by: Winkler, R., German Federal Ministry of Education and Research (BMBF), Publications and Website Division, Berlin, Germany, 265 pp., 2005.

ATMOFAST: Atmosphärischer Ferntransport und seine Auswirkungen auf die Spurengaskonzentrationen in der freien Troposphäre über Mitteleuropa (Atmospheric Long-range Transport and its Impact on the Trace-gas Composition of the Free Troposphere over Central Europe), Project Final Report, T. Trickl, Co-ordinator, M. Kerschgens, A. Stohl, and T. Trickl, subproject co-ordinators, funded by the German Ministry of Education and Research within the programme "Atmosphärenforschung 2000" (in German), 130 pp., 2005.

Austin, J. F. and Midgley, R. P.: The Climatology of the jet stream and stratospheric intrusions of ozone over Japan, Atmos. Environ., 28, 39–52, 1994.

Beirle, S., Spichtinger, N., Stohl, A., Cummins, K. L., Turner, T., Boccippio, D., Cooper, O. R., Wenig, M., Grzegorski, M., Platt, U., and Wagner, T.: Estimating the NO_x produced by lightning from GOME and NLDN data: a case study in the Gulf of Mexico, Atmos. Chem. Phys., 6, 1075–1089, doi:10.5194/acp-6-1075-2006, 2006.

Bithell, M., Vaughan, G., and Gray, L. J.: Persistence of stratospheric ozone layers in the troposphere, Atmos. Environ., 34, 2563–2570, 2000.

Cammas, J.-P., Jacoby-Koaly, S., Suhre, K., Rosset, R., and Marenco, A.: Atlantic subtropical potential vorticity barrier of Ozone by Airbus In-Service Aircraft (MOZAIC) flights, J. Geophys. Res., 103, 25681–25693, 1998.

Carnuth, W., Kempfer, U., and Trickl, T.: Highlights of the Tropospheric Lidar Studies at IFU within the TOR Project, Tellus B, 54, 163–185, 2002.

Claude, H., Steinbrecht, W., and Köhler, U.: Entwarnung bei der Ozonschicht, Ozonbulletin des Deutschen Wetterdiensts, available from http://www.dwd.de, 119, 2, 2008 (in German).

Cooper, O. R., Forster, C., Parrish, D., Trainer, M., Dunlea, E., Ryerson, T., Hübler, G., Fehsenfeld, F., Nicks, D., Holloway, J., de Gouw, J., Warneke, C., Roberts, J. M., Flocke, F., and

ACPD
10, 30473–30537, 2010

Moody, J.: A case study of transpacific warm conveyor belt transport: Influence of merging airstreams on trace gas import to North America, J. Geophys. Res., 109, D23S08, doi:10.1029/2003JD003624, 2004a.

Cooper, O., Forster, C., Parrish, D., Dunlea, E., Hübler, G., Fehsenfeld, F., Holloway, J., Oltmans, S., Johnson, B., Wimmers, A., and Horowitz, L.: On the life cycle of a stratospheric intrusion and its dispersion into polluted warm conveyor belts, J. Geophys. Res., 109, D23S09, doi:10.1029/2003JD00400618, 2004b.

Cooper, O. R., Stohl, A., Hübler, G., Hsie, E. Y., Parrish, D. D., Tuck, A. F., Kiladis, G. N:, Oltmans, S. J., Johnson, B. J., Shapiro, M., Moody, J. L, and Lefohn, A. S.: Direct transport of midlatitude stratospheric ozone into the lower troposphere and marine boundary layer of the tropical Pacific Ocean, J. Geophys. Res., 100, D23310, doi:10.1029/2005JD005783, 2005.

Cooper, O. R., Stohl, A., Trainer, M., Thompson, A. M., Witte, J. C., Oltmans, S. J., Morris, G., Pickering, K. E., Crawford, J. H., Chen, G., Cohen, R. C., Bertram, T. H., Wooldridge., P., Perring, A., Brune, W. H., Merrill, J., Moody, J. L., Tarasick, D., Nédélec, P., Forbes, G., Newchurch, M. J., Schmidlin, F. J., Johnson, B. J., Turquety, S., Baughcum, S. L., Ren, X., Fehsenfeld, F. C., Meagher, J. F., Spichtinger, N., Brown, C. C., McKeen, S. A., McDermid, I. S., and Leblanc, T.: Large upper tropospheric ozone enhancements above midlatitude North America during summer: In situ evidence from the IONS and MOZAIC ozone measurements network, J. Geophys. Res. 111, D24S05, doi:10.1029/2006JD007306, 2006.

Cristofanelli, P., Bonasoni, P., Collins, W., Feichter, J., Forster, C., Kentarchos, A., Kubik, P. W., James, P., Land, C., Meloen, J., Roelofs, G. J., Siegmund, P., Sprenger, M., Schnabel, C., Stohl, A., Tositti, L., Trickl, T., Wernli, H., and Zanis, P.: Stratosphere to troposphere transport: a model and method evaluation, J. Geophys. Res., 108, 8525, doi:10.1029/2002JD002600, 2003.

Danielsen, E. F.: Stratospheric-Tropospheric Exchange Based on Radioactivity, Ozone and Potential Vorticity, J. Atmos. Sci., 25, 502-518, 1968.

Davis, T. D. and Schuepbach, E.: Episodes of high ozone concentrations at the earth's surface resulting from transport down from the upper troposphere/lower stratosphere: a review and case studies, Atmos. Environ., 28, 53–68, 1994.

Deshler, T., Anderson-Sprecher, R., Jäger, H., Barnes, J., Hofmann, D. J., Clemensha, B., Simonich, D., Grainger, R. G., and Godin-Beekmann, S.: Trends in the non-volcanic component of stratospheric aerosol over the period 1971–2004, J. Geophys. Res., 111, D01201,

ACPD
10, 30473–30537, 2010

doi:10.1029/2005JD00608, 2006.
Ding, A. J., Wang, T., Thouret, V., Cammas, J.-P., and Nédélec, P.: Tropospheric ozone climatology over Beijing: analysis of aircraft data from the MOZAIC program, Atmos. Chem. Phys., 8, 1–13, doi:10.5194/acp-8-1-2008, 2008.
Eisele, H. and Trickl, T.: Second Generation of the IFU Stationary Tropospheric Ozone Lidar, in: Advances in Atmospheric Remote Sensing with Lidar, Selected Papers of the 18th International Laser Radar Conference, Berlin (Germany), July 22 to 26, 1996, edited by: Ansmann, A., Neuber, R., Rairoux, P., Wandinger, U., Springer, Berlin, Heidelberg, Germany, 79–382, 1997.
Eisele, H. and Trickl, T.: Improvements of the aerosol algorithm in ozone-lidar data processing by use of evolutionary strategies, Appl. Optics, 44, 2638–2651, 2005.
Eisele, H., Scheel, H. E., Sladkovic, R., and Trickl, T.: High-resolution Lidar Measurements of Stratosphere-troposphere Exchange, J. Atmos. Sci., 56, 319–330, 1999.
Elbern, H., Kowol, J., Sladkovic, R., and Ebel, A.: Deep stratospheric intrusions: A statistical assessment with model guided analysis, Atmos. Environ., 31, 3207–3226, 1997.
Emanuel, K. A. and Živković-Rothman, M.: Development and evaluation of a convection scheme for use in climate models, J. Atmos. Sci., 56, 1766-1782, 1999.
Fehsenfeld, F. C., Ancellet, G., Bates, T. S., Goldstein, A. H., Hardesty, R. M., Honrath, R., Law, K. S., Lewis, A. C., Leaitch, R., McKeen, S., Meagher, J., Parrish, D. D., Pszenny, A. A. P., Russell, P. B., Schlager, H., Seinfeld, J., Talbot, R., and Zbinden, R.: International consortium for atmospheric research on transport and transformation (ICARTT): North America to Europe – Overview of the 2004 summer field study, J. Geophys. Res., 111, D23S01, doi:10.1029/2006JD007829, 2006.
Feldmann, H., Memmesheimer, M., Ebel, A., Seibert, P., Wotawa, G., Kromp-Kolb, H., Trickl, T., and Prévôt, A.: Evaluation of a Regional Scale Model for the Alpine Region with Data from the VOTALP Project, in: Proceedings of EUROTRAC Symposium 1998, Garmisch-Partenkirchen (Germany), March 23–17, 1998, edited by: Borrell, P. M. and Borrell, P., WIT-press, Southampton, UK, 483–488, 1999.
Folkins, I. and Appenzeller, C.: Ozone and potential vorticity at the subtropical tropopause break, J. Geophys. Res., 101, 18787-18792, 1996.
Forster, C., Wandinger, U., Wotawa, G., James, P., Mattis, I., Althausen, D., Simmonds, P., O'Doherty, S., Jennings, S. G., Kleefeld, C., Schneider, J., Trickl, T., Kreipl, S., Jäger, H., and Stohl, A.: Transport of boreal forest fire emissions from Canada to Europe, J. Geophys. Res.,

ACPD
10, 30473–30537, 2010

106, 22887–22906, 2001.
Forster, C., Stohl, A., and Seibert, P.: Parameterization of convective transport in a Lagrangian particle dispersion model and its valuation, J. Appl. Meteor. Clim., 46, 403-422, 2007.
Freudenthaler, V., Homburg, F., and Jäger, H.: Ground-based mobile scanning LIDAR for remote sensing of contrails, Ann. Geophys., 12, 956–961, doi:10.5194/angeo-12-956-1994, 1994.
Freudenthaler, V., Homburg, F., and Jäger, H.: Contrail observations by ground-based mobile scanning lidar: cross-sectional growth, Geophys. Res. Lett., 22, 3501–3504, 1995.
Fromm, M., Shettle, E. P., Fricke, K. H., Ritter, C., Trickl, T., Giehl, H., Gerding, M., Barnes, J., O'Neill, M., Massie, S. T., Blum, U., McDermid, I. S., Leblanc, T., and Deshler, T.: The stratospheric impact of the Chisholm PyroCumulonimbus eruption: 2. Vertical profile perspective, J. Geophys. Res., 113, D08203, doi:10.1029/2007JD009147, 2008.
Fromm, M., Lindsey, D. T., Servranckx, R., Yue, G., Trickl, T., Sica, R., Doucet, P., and Godin-Beekmann, S.: The Untold Story of Pyrocumulonimbus, Bull. Am. Meterol. Soc., 91, 1193-1209, 2010.
Frost, G. J., McKeen, S. A., Trainer, M., Ryerson, T. B., Neuman, J. A., Roberts, J. M., Swanson, A., Holloway, J. S., Sueper, D. T., Parrish, D. D., Fehsenfeld, F. C., Flocke, F., Peckham, S. E., Grell, G. A., Kowal, D., Cartwright, J., Auerbach, N., and Habermann, T.: Effects of changing power plant NO_x emissions on ozone in the eastern United States: Proof of concept, J. Geophys. Res., 111, D12306, doi:10.1029/2005JD006354, 2006.
Gouget, H., Cammas, J.-P., Marenco, A., Rosset, R., and Jonquières, I.: Ozone peaks associated with a subtropical tropopause fold and with the trade wind inversion: A case study from the airborne campaign TROPOZ II over the Caribbean in winter, J. Geophys. Res., 101, 25979–25993, 1996.
Grousset, F. E., Ginoux, P., Bory, A., and Biscaye, P. E.: Case study of a Chinese dust plume reaching the French Alps, Geophys. Res. Lett., 30, 1277, doi:10.1029/2002GL016833, 2003.
Huntrieser, H., Heland, J., Schlager, H., Forster, C., Stohl, A., Aufmhoff, H., Arnold, F., Scheel, H. E., Campana, M., Gilge, S., Eixmann, R., and Cooper, O.: Intercontinental air pollution transport from North America to Europe: Experimental evidence from aircraft measurements and surface observations, J. Geophys. Res., 110, DO1305, doi:10.1029/2004JD005045, 2005.
Huntrieser, H., Schlager, H., Roiger, A., Lichtenstern, M., Schumann, U., Kurz, C., Brunner, D.,

ACPD
10, 30473–30537, 2010

Schwierz, C., Richter, A., and Stohl, A.: Lightning-produced NO_x over Brazil during TROCCINOX: airborne measurements in tropical and subtropical thunderstorms and the importance of mesoscale convective systems, Atmos. Chem. Phys., 7, 2987–3013, doi:10.5194/acp-7-2987-2007, 2007.

Jäger, H.: Long-term record of lidar observations of the stratospheric aerosol layer at Garmisch-Partenkirchen, J. Geophys. Res., 110, D08106, doi:10.1029/2004JD005506, 2005.

Jäger, H., Carnuth, W., and Georgi, B.: Observations of Saharan Dust at a North Alpine Station, J. Aerosol Sci., 19, 1235–1238, 1988

Jäger, H., Kreipl, S., James, P., Stohl, A., and Trickl, T.: Long-range Transport and its Impact on the Vertical Distribution of Trace Constitutents in the Central European Free Troposphere, in: Reviewed and Revised Papers Presented at the 22nd International Laser Radar Conference, Matera, Italy, July 12 to 16, 2004, edited by: Pappalardo, G., Amodeo, A., and Warmbein, B., ESA Publications Division, Noordwijk, The Netherlands, ISBN 92-9092-872-7, ISSN 0379-6566, 679–682, 2004.

Jäger, H., James, P., Stohl, A., and Trickl, T: Long-Range Transport of Free-Tropospheric Aerosol: A Nine-year Climatology, in: Reviewed and Revised Papers Presented at the 23rd International Laser Radar Conference, Nara (Japan), July 24 to 28, 2006, edited by: Nagasawa, C., Sugimoto, N., Tokyo Metropolitan University, Tokyo, Japan, ISBN 4-9902916-0-3795–796, 2006.

James, P., Stohl, A., Forster, C., Eckhardt, S, Seibert, P., and Frank, A.: A 15-year climatology of stratosphere-troposphere exchange with a Lagrangian particle dispersion model, 2. Mean climate and seasonal variability, J. Geophys. Res., 108, 8522, doi:10.1029/2002JD002639, 2003.

Kanter, H.-J., Scheel, H. E., Trickl, T., James, P., Stohl, A., and Feldmann, H.: Atmospheric Long-range Transport and its Impact on the Trace-gas Distribution in the Free Troposphere over Central Europe (ATMOFAST), in: Ozone, Proceedings of the XXth Quadrennial Ozone Symposium, Kos (Greece), 1 to 8 June 2004, edited by: Zerefos, C., University of Athens (Athens, Greece, 2004)/International Ozone Commission, Genève, Switzerland, ISBN 960-630-103-6, ISBN 960-630-105-2, 849–850, 2004.

Kempfer, U., Carnuth, W., Lotz, R., and Trickl, T.: A wide-range UV lidar system for tropospheric ozone measurements: development and application, Rev. Sci. Instrum., 65, 3145–3164, 1994.

Keyser, D. and Shapiro, M. A.: A Review of the Structure and Dynamics of Upper-Level Frontal

ACPD
10, 30473–30537, 2010

Zones, Mon. Weather Rev. 114, 452-499, 1986.
Koch, P., Wernli, H., and Davies, H. C.: An Event-based Jet-stream Climatology and Typology, Int. J. Climatol., 26, 283–301, 2006.
Komhyr, W. D.: Electrochemical concentration cells for gas analysis, Ann. Geophys., 25, 203–210, 1969.
Kreipl, S., Mücke, R., Jäger, H., Trickl, T., and Stohl, A.: Spectacular Cases of Vertical and Long-range Ozone and Aerosol Transport, in: Laser Remote Sensing of the Atmosphere, Selected Papers of the 20th International Laser Radar Conference, Vichy (France), 10 to 14 July 2000, edited by: Dabas, A., Pelon, J., Éditions de l'École Polytechnique, Paris, France, 455–458, 2001.
Krishnamurti, T. N.: The Subtropical Jet Stream of Winter, J. Meteor., 18, 172–191, 1961.
Kritz, M. A., Le Roulley, J.-C., and Danielsen, E. F.: The China Clipper – fast advective transport of radon-rich air from the Asian boundary layer to the upper troposphere near California, Tellus B, 42, 46–61, 1990.
Law, K. S., Penkett, S. A., Reeves, C. E., Evans, M. J., Pyle, J. A., Bauguitte, S., Green, T. J., Bandy, B., Mills, G. P., Barjat, H., Kley, D., Schmitgen, S., Monks, P. S., Edwards, G. D., Kent J. M., Dewey, K., and Kaye, A.: Evidence for anthropogenic influence over the central North Atlantic. IGACtivities, International Global Atmospheric Chemistry, Newsletter 24, 17–19, 2001.
Liang, Q., Jaeglé, L., Hudman, R. C., Turquety, S., Jacob, D. J., Avery, M. A., Browell, E. V., Sachse, G. W., Blake, D. R., Brune, W., Ren, X., Cohen, R. C., Dibb, J. E., Fried, A., Fuelberg, H., Porter, M., Heikes, B. G., Huey, G., Singh, H. B., and Wennberg, P. O.: Summertime influence of Asian pollution in the free troposphere over North America, J. Geophys. Res., 112, D12S11, doi:10.1029/2006JD007919, 2007.
Ma, J. and van Aardenne, J. A.: Impact of different emission inventories on simulated tropospheric ozone over China: a regional chemical transport model evaluation, Atmos. Chem. Phys., 4, 877–887, doi:10.5194/acp-4-877-2004, 2004.
Marenco, A., Thouret, V., Nédélec, P., Smit, H., Helten, M., Kley, D., Karcher, F., Simon, P., Law, K., Pyle, J., Poschmann, G., von Wrede, R., Hume, C., and Cook, T.: Measurement of ozone and water vapor by Airbus in-service aircraft: The MOZAIC airborne program, An overview, J. Geophys. Res., 103, 25631–25642, 1998.
Meloen, J., Siegmund, P., van Velthoven, P., Kelder, H., Sprenger, M., Wernli, H., Kentarchos, A., Roelofs, G., Feichter, J., Land, C., Forster, C., James, P., Stohl, A., Collins, B.,

ACPD
10, 30473–30537, 2010

and Cristofanelli, P.: Stratosphere troposphere exchange: a model and method intercomparison, J. Geophys. Res., 108, 8526, doi:10.1029/2002JD002274, 2003.
Newell, R. E., Thouret, V., Cho, J. Y. N., Stoller, P., Marenco, A., and Smit, H. G.: Ubiquity of quasi-horizontal layers in the troposphere, Nature, 198, 316–319, 1999.
Olivier, J. G. J. and Berdowski, J. J. M.: Global emissions sources and sinks, in: The Climate System, edited by: Berdowski, J., Guicherit, R., Heij, B. J., A. A. Balkema Publishers/Swets & Zeitlinger Publishers, Lisse, The Netherlands, ISBN 90 5809 255 0, 33–78, 2001.
Papayannis, A., Amiridis, V., Mona, L., Tsaknakis, G., Balis, D., Bösenberg, J., Chaikovski, A., De Tomasi, F., Grigorov, I., Mattis, I., Mitev, V., Müller, D., Nickovic, S., Pérez, C., Pietruczuk, A., Pisani, G., Ravetta, F., Rizi, V., Sicard, M., Trickl, T., Wiegner, M., Gerding, M., Mamouri, R. E., D'Amico, G., and Pappalardo, G.: Systematic lidar observations of Saharan dust over Europe in the frame of EARLINET (2000–2002), J. Geophys. Res., 113, D10204; doi:10.1029/2007JD009028, 2008.
Penkett, S. A., Evans, M. J., Reeves, C. E., Law, K. S., Monks, P. S., Bauguitte, S. J. B., Pyle, J. A., Green, T. J., Bandy, B. J., Mills, G., Cardenas, L. M., Barjat, H., Kley, D., Schmitgen, S., Kent, J. M., Dewey, K., and Methven, J.: Long-range transport of ozone and related pollutants over the North Atlantic in spring and summer, Atmos. Chem. Phys. Discuss., 4, 4407–4454, doi:10.5194/acpd-4-4407-2004, 2004.
Prados, A. I., Dickerson, R. R., Doddrige, B. G., Milne, P. A., Moody, J. L., and Merrill J. T.: Transport of ozone and pollutants to the North Atlantic Ocean during the 1996 Atmosphere/Ocean Chemistry Experiment (AEROCE) intensive, J. Geophys. Res., 104, 26219–26233, 1999.
Reiter, R., Sladkovic, R., Pötzl, K., Carnuth, W., and Kanter, H.-J.: Studies of the influx of stratospheric air into the lower troposphere using cosmic-ray-produced radionuclides and fallout, Arch. Meteor. Geophy. A, 20A, 211–246, 1971.
Reiter, R., Sladkovic, R., and Kanter, H.-J.: Concentration of trace gases in the lower troposphere, simultaneously recorded at neighboring mountain stations, Part II: ozone, Meteorol. Atmos. Phys., 37, 27–47, 1987.
Richter, A., Burrows, J. P., Nüß, H., Granier, C., and Niemeier, U.: Increase in tropospheric nitrogen dioxide over China oberved from Space, Nature, 437, 129–132, 2005.
Roelofs, G. J., Kentarchos, A. S., Trickl, T., Stohl, A., Collins, W. J., Crowther, R. A., Hauglustaine, D., Klonecki, A., Law, K. S., Lawrence, M. G., von Kuhlmann, R., and van Weele, M.: Intercomparison of tropospheric ozone models: Ozone transport in a complex tropopause

ACPD
10, 30473–30537, 2010

folding event, J. Geophys. Res., 108, 8529, doi:10.1029/2003JD003462, 2003.
Schuepbach, E., Davies, T. D., Massacand, A. C., and Wernli, H.: Mesoscale modelling of vertical atmospheric transport in the Alps associated with the advection of a tropopause fold – a winter ozone episode, Atmos. Environ., 33, 3613–3626, 1999.
Schumann, U. and Huntrieser, H.: The global lightning-induced nitrogen oxides source, Atmos. Chem. Phys., 7, 3823–3907, doi:10.5194/acp-7-3823-2007, 2007.
Seibert, P., Feldmann, H., Neininger, B., Bäumle, M., and Trickl, T.: South foehn and ozone in the Eastern Alps – case study and climatological aspect, Atmos. Environ., 34, 1379–1394, 2000.
Seibert, P. and Frank, A.: Source-receptor matrix calculation with a Lagrangian particle dispersion model in backward mode, Atmos. Chem. Phys., 4, 51-63, doi:10.5194/acp-4-51-2004, 2004.
Singh, H. B., Salas, L., Herlth, D., Kolyer, R., Czech, E., Avery, M., Crawford, J. H., Pierce, R. B., Sachse, G. W., Blake, D. R., Cohen, R. C., Bertram, T. H., Perring, A., Wooldridge, P. J., Dibb, J., Huey, G., Hudman, R. C., Turquety, S., Emmons, L. K., Flocke, F., Tang, Y., Carmichael, G. R., and Horowitz, L. W.: Reactive nitrogen distribution and partitioning in the North American troposphere and lowermost stratosphere, J. Geophys. Res. 112, D12S04, doi:10.1029/2006JD007664, 2007.
Sioris, C. E., McLinden, C. A., Martin, R. V., Sauvage, B., Haley, C. S., Lloyd, N. D., Llewellyn, E. J., Bernath, P. F., Boone, C. D., Brohede, S., and McElroy, C. T.: Vertical profiles of lightning-produced NO_2 enhancements in the upper troposphere observed by OSIRIS, Atmos. Chem. Phys., 7, 4281–4294, doi:10.5194/acpd-7-4281-2007, 2007.
Sprenger, M. and Wernli, H.: A northern hemisphere climatology of cross-tropopause exchange for the ERA 15 time period, J. Geophys. Res., 108, 8521, doi: 10.1029/2002JD002636, STA 6, 14 pp., 2003.
Sprenger, M., Croci Maspoli, M., and Wernli, H.: Tropopause folds and cross-tropopause exchange: A global investigation based upon ECMWF analyses for the time period March 2000 to February 2001, J. Geophys. Res., 108, 8518, doi:10.1029/2002JD002587, 2003.
Stohl, A.: A 1-year Lagrangian "climatology" of airstreams in the Northern Hemisphere troposphere and lowermost stratosphere, J. Geophys. Res., 106, 7263–7279, 2001.
Stohl, A. and Seibert, P.: Accuracy of trajectories as determined from the conservation of meteorological tracers, Q. J. Roy. Meteor. Soc., 124, 1465–1484, 1998.
Stohl, A. and Thomson, D. J.: A density correction for Lagrangian particle dispersion models,

ACPD
10, 30473–30537, 2010

Bound.-Lay. Meteorol., 90, 155–167, 1999.
Stohl, A. and Trickl, T.: A textbook example of long-range transport: Simultaneous observation of ozone maxima of stratospheric and North American origin in the free troposphere over Europe, J. Geophys. Res., 104, 30445–30462, 1999.
Stohl, A., Wotawa, G., Seibert, P., and Kromp-Kolb, H.: Interpolation errors in wind fields as a function of spatial and temporal resolution and their impact on different types of kinematic trajectories, J. Appl. Meteorol., 34, 2149–2165, 1995.
Stohl, A., Hittenberger, M., and Wotawa, G.: Validation of the Lagrangian particle dispersion model FLEXPART against large scale tracer experiments, Atmos. Environ., 32, 4245–4264, 1998.
Stohl, A., Spichtinger-Rakowsky, N., Bonasoni, P., Feldmann, H., Memmesheimer, M., Scheel, H. E., Trickl, T., Hübener, S., Ringer, W., and Mandl, M.: The influence of stratospheric intrusions on alpine ozone concentrations, Atmos. Environ., 34, 1323–1354, 2000.
Stohl, A., Eckhardt, S., Forster, C., James, P., Spichtinger, N., and Seibert, P.: A replacement for simple back trajectory calculations in the interpretation of atmospheric trace substance measurements, Atmos. Environ., 36, 4635–4648, 2002.
Stohl, A., Eckhardt, S., Spichtinger, N., Huntrieser, H., Heland, J., Schlager, H., Wilhelm, S., Arnold, F., and Cooper, O.: A backward modelling study of intercontinental transport using aircraft measurements, J. Geophys. Res., 108, 4370, doi:10.1029/2002JD002862, 2003.
Stohl, A., Forster, C., Frank, A., Seibert, P., and Wotawa, G.: Technical note: The Lagrangian particle dispersion model FLEXPART version 6.2, Atmos. Chem. Phys., 5, 2461–2474, doi:10.5194/acpd-5-2461-2005, 2005.
Stohl, A., Forster, C., Huntrieser, H., Mannstein, H., McMillan, W. W., Petzold, A., Schlager, H., and Weinzierl, B.: Aircraft measurements over Europe of an air pollution plume from Southeast Asia – aerosol and chemical characterization, Atmos. Chem. Phys., 7, 913–937, doi:10.5194/acpd-7-913-2007, 2007.
Thouret, V., Cammas, J.-P., Sauvage, B., Athier, G., Zbinden, R., Nédélec, P., Simon, P., and Karcher, F.: Tropopause referenced ozone climatology and inter-annual variability (1994–2003) from the MOZAIC programme, Atmos. Chem. Phys., 6, 1033–1051, doi:10.5194/acpd-6-1033-2006, 2006.
Trickl, T., Cooper, O. C., Eisele, H., James, P., Mücke, R., and Stohl, A.: Intercontinental transport and its influence on the ozone concentrations over central Europe: Three case studies, J. Geophys. Res., 108, 8530, doi:10.1029/2002JD002735, 2003.

ACPD
10, 30473–30537, 2010

Trickl, T., Bärtsch-Ritter, N., Eisele, H., Furger, M., Mücke, R., and Stohl, A.: High-ozone layers in the middle and upper troposphere above Central Europe: strong import from the stratosphere over the Pacific Ocean, Atmos. Chem. Phys. Discuss., 9, 3113–3166, doi:10.5194/acpd-9-3113-2009, 2009.

Trickl, T., Feldmann, H., Kanter, H.-J., Scheel, H.-E., Sprenger, M., Stohl, A., and Wernli, H.: Forecasted deep stratospheric intrusions over Central Europe: case studies and climatologies, Atmos. Chem. Phys., 10, 499–524, doi:10.5194/acp-10-499-2010, 2010.

Vogelmann, H. and Trickl, T.: Wide-range sounding of free-tropospheric water vapor with a differential-absorption lidar (DIAL) at a high-altitude station, Appl. Optics, 47, 2116–2132, 2008.

VOTALP II: Vertical Ozone Transport in the Alps II, Final Report for the European Union, Contract Nr.: ENV4 CT970413, Reporting Period 1/3/1998-29/2/2000, H. Kromp-Kolb, Coordinator, Universität für Bodenkultur Wien (Austria), Institut für Meteorologie und Physik, http://www.boku.ac.at/imp/votalp/, 96 pp., 2000.

Wernli, H. and Davies, H. C.: A Lagrangian-based analysis of extratropical cyclones. I. The method and some applications, Q. J. Roy. Meteorol. Soc., 123, 467–489, 1997a.

Wernli, H.: A Lagrangian-based analysis of extratropical cyclones. II: A detailed case study, Q. J. Roy. Meteorol. Soc., 123, 1677–1706, 1997b.

Wernli, H. and Bourqui, M.: A Lagrangian ,“one-year climatology” of (deep) cross-tropopause in the extratropical northern hemisphere, J. Geophys. Res., 107, 4021, doi:10.1029/2001JD000812, 16 pp., 2002.

Zanis, P., Trickl, T., Stohl, A., Wernli, H., Cooper, O., Zerefos, C., Gaeggeler, H., Schnabel, C., Tobler, L., Kubik, P. W., Priller, A., Scheel, H. E., Kanter, H. J., Cristofanelli, P., Forster, C.,James, P., Gerasopoulos, E., Delcloo, A., Papayannis, A., and Claude, H.: Forecast, observation and modelling of a deep stratospheric intrusion event over Europe, Atmos. Chem. Phys., 3, 763–777, doi:10.5194/acp-3-763-2003, 2003.

ACPD
10, 30473–30537, 2010

Table 1. Overview of the high-ozone layers analysed.

Case	Start Date	Duration	Typ. Vert. Range	O_3 Mix. Ratio	Asian Influence	Aerosol
1	31 May 1996	≥21 h	4.5–7.5 km	80–100 ppb	no	no
		unknown	7.5–11 km	80 ppb	no	low
2	26 May 1999	>4 d	4.5–9 km	80–150 ppb	yes	strong
3	9 Sept. 2000	>15 h	7–10 km	80–110 ppb	no	no
4	23 June 2001	≥2 d	5.512 km	70110 ppb	no	no
5	22 July 2001	1.5 d	5.5–8 km	70–90 ppb	low	no
		>0.5 d	8–10 km	100–120 ppb	low	no
6	13 August 2001	>3 d	6–11 km	100–140 ppb	no	no

ACPD
10, 30473–30537, 2010

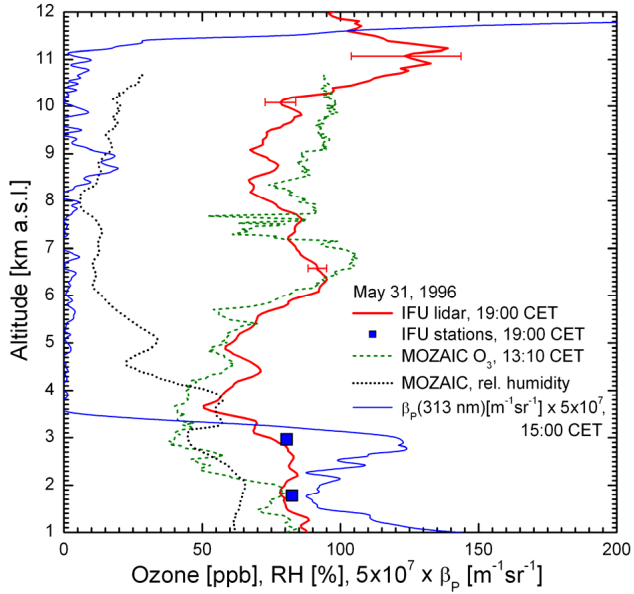

Fig. 1. Ozone mixing ratio and 313-nm aerosol backscatter coefficient β_P above IMK-IFU (Garmisch-Partenkirchen) and MOZAIC ozone and relative-humidity (RH) profiles for the departure of a MOZAIC aeroplane from Frankfurt (Germany); see Fig. 12 in (Trickl et al., 2003). The ozone mixing ratios of the nearby summit stations Wank (1780 m a.s.l.) and Zugspitze (2962 m) are also given for comparision. The ozone peak at 11 km is a temporary feature and somewhat uncertain due to the presence of cirrus clouds just below the tropopause (13.4 km±0.2 km during 31 May). The times are given in Central European Time (CET = UTC + 1 h).

ACPD
10, 30473–30537, 2010

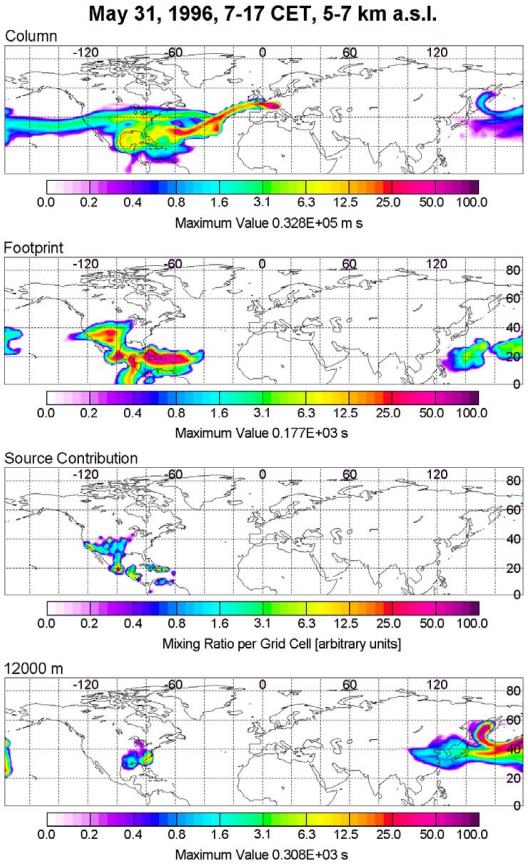

Fig. 2. FLEXPART fifteen-day backward (retroplume) simulation for 31 May 1996, 07:00 to 17:00 CET and 5 to 7 km a.s.l. above IMK-IFU; the PBL source contribution was determined by folding the footprint emission sensitivity with NO_x emissions from the EDGAR inventory.

ACPD
10, 30473–30537, 2010

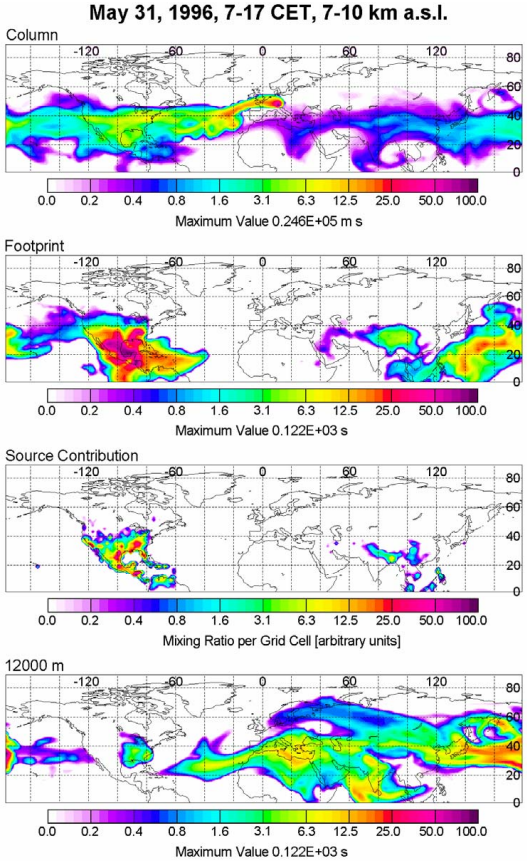

Fig. 3. Same as Fig. 2, but for the altitude range 7 to 10 km a.s.l. above IMK-IFU.

ACPD
10, 30473–30537, 2010

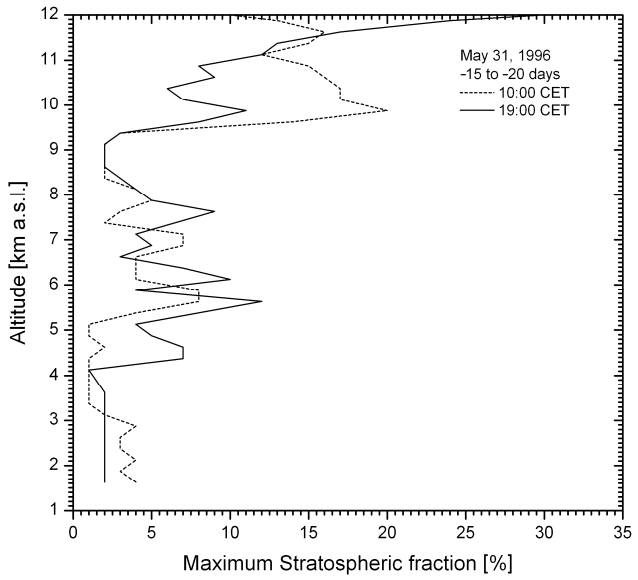

Fig. 4. Vertical distribution of the maximum stratospheric fraction in the twenty-day retroplumes calculated for the four measurements in Fig. 1, extracted from the results for days −20 to −15, for which, though slightly outside the ozone maximum in Fig. 1, the highest fractions were obtained.

ACPD
10, 30473–30537, 2010

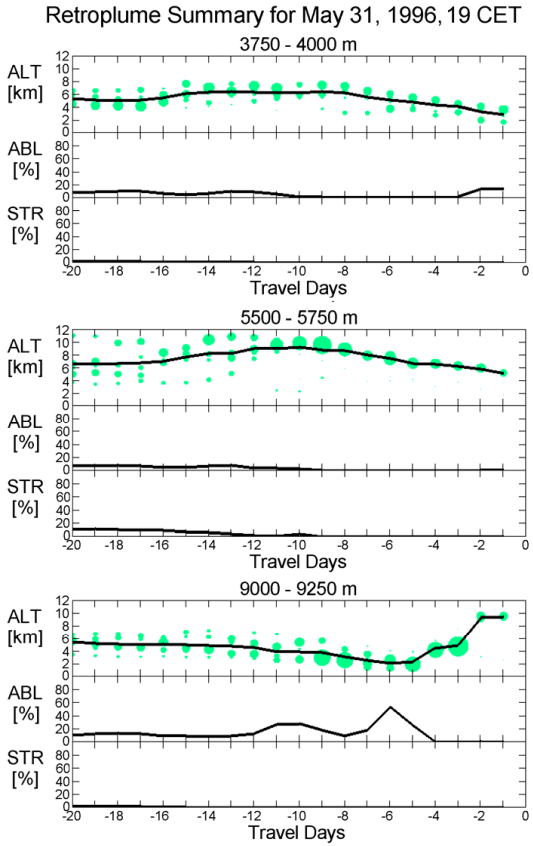

Fig. 5. Retroplume summaries for three selected altitude ranges above Garmisch-Partenkirchen initiated at the time of the lidar measurement in Fig. 1. The panels show the approximate vertical position (ALT: altitude) of the backward plume during the preceding 20 days and the relative single-day contributions from the PBL (ABL) and the stratosphere (STR). For details see Sect. 2.2.

ACPD
10, 30473–30537, 2010

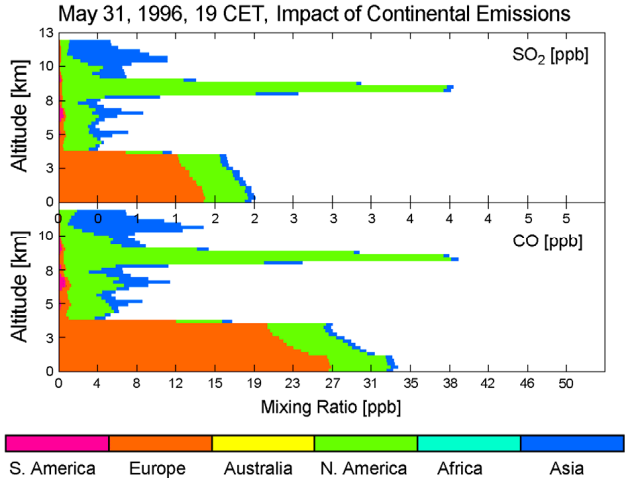

Fig. 6. Vertical distribution of SO_2 and CO emission tracers from the different source continents above Garmisch-Partenkirchen, simulated for the time of the lidar measurement on 31 May 1996 shown in Fig. 1. Please, note that the numbers in the mixing-ratio scales are just rounded to the next integer value.

ACPD
10, 30473–30537, 2010

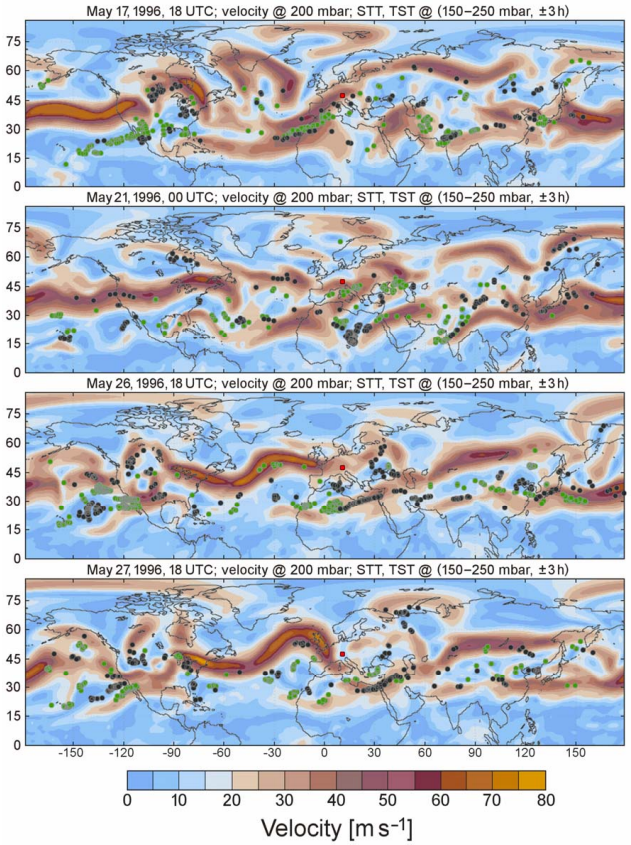

Fig. 7. Selected examples of the LAGRANTO visualizations of the jet streams for Case 1; the position of Garmisch-Partenkirchen is marked with a red dot next to the centre of each panel. The positions where trajectories revealed STT or TST between 150 and 200 mbar are marked by green and black dots, respectively.

ACPD
10, 30473–30537, 2010

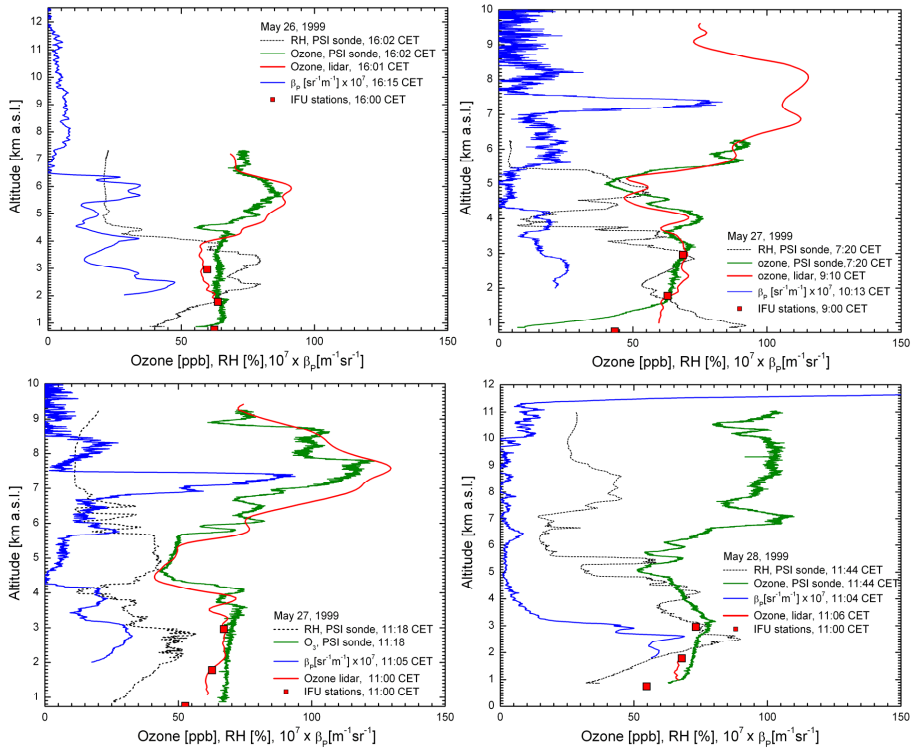

Fig. 8. Examples of lidar, sonde and station measurements from the VOTALP II "Munich" field campaign, **(a)** 26 May 1999, around 16:00 CET; **(b)** in the morning of 27 May 1999; **(c)** around noon on 27 May 1999; **(d)** before noon on 28 May 1999. Shown are ozone (from lidar, PSI sonde, stations), relative humidity (RH, from PSI sonde) and the aerosol backscatter coefficient β_P derived from the measurements with the "NDACC" aerosol lidar at large elevation angles of at least 45°.

ACPD
10, 30473–30537, 2010

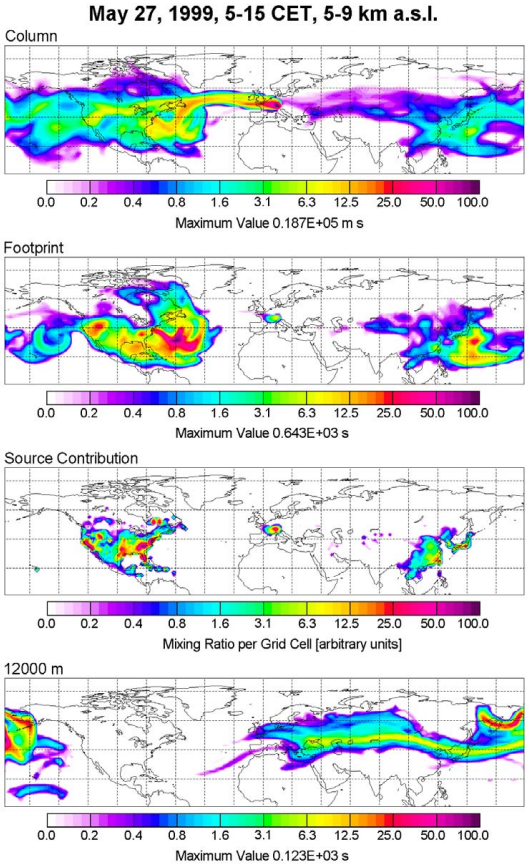

Fig. 9. Fifteen-day backward simulation with FLEXPART for 27 May 1999, between 05:00 and 15:00 CET, corresponding to the measurements in Fig. 8b and c.

ACPD
10, 30473–30537, 2010

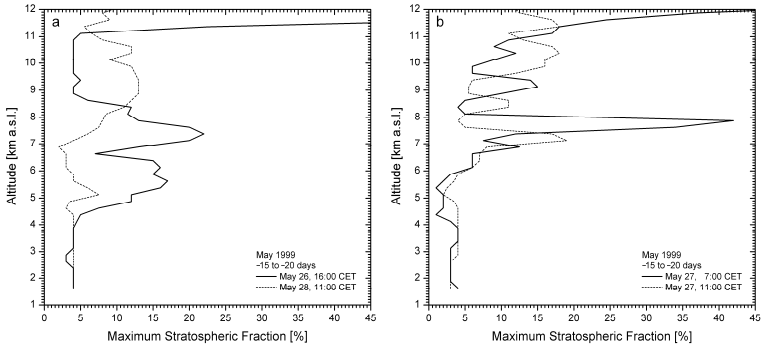

Fig. 10. Vertical distribution of the maximum stratospheric fraction in the twenty-day FLEXPART retroplumes calculated for the four measurements in Fig. 7, extracted from days −20 to −15: **(a)** 26 May and 28 May, **(b)** 27 May.

ACPD
10, 30473–30537, 2010

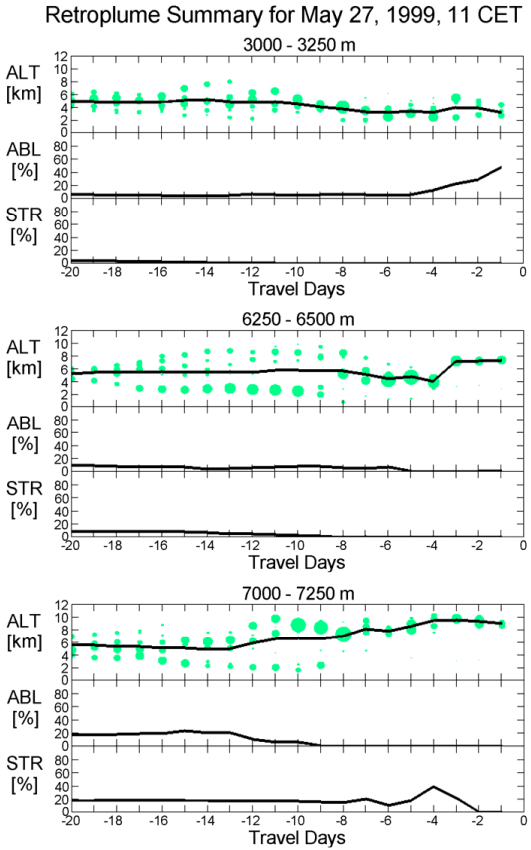

Fig. 11. Retroplume time-height sections for three selected altitude ranges above Garmisch-Partenkirchen initiated at the time of the lidar measurement in Fig. 8c; for details see Fig. 5 and Sect. 2.2. The simulations for Fig. 8b look similar.

ACPD
10, 30473–30537, 2010

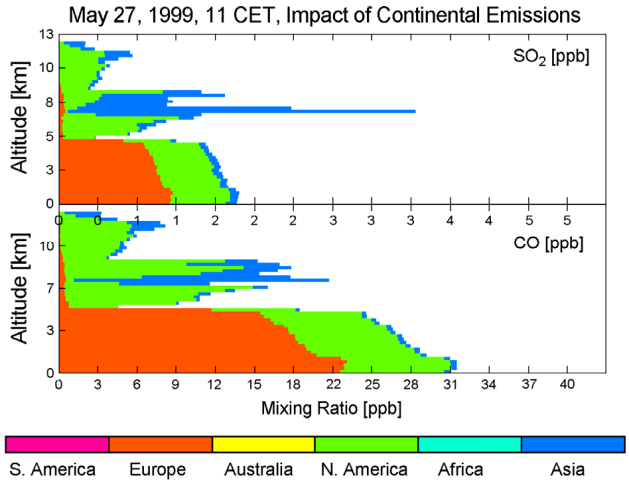

Fig. 12. Vertical distribution of SO_2 and CO emission tracers from the different source continents above Garmisch-Partenkirchen, calculated for the time of the lidar measurement on 27 May 1999, shown in Fig. 8c; Asian influence is found in the altitude range around 8 km.

ACPD
10, 30473–30537, 2010

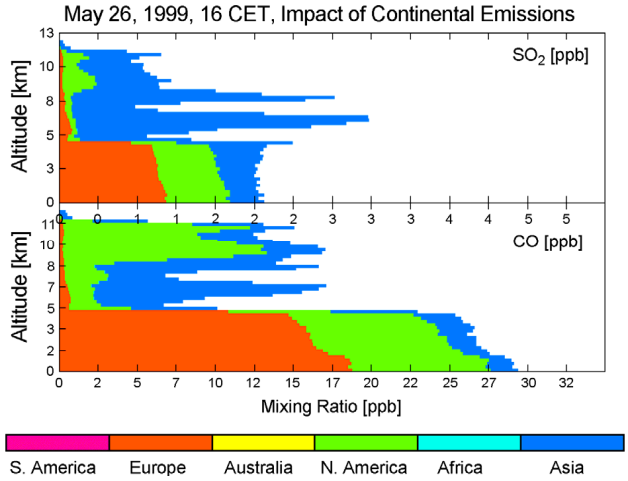

Fig. 13. Vertical distribution of SO_2 and CO emission tracers from the different source continents calculated for the lidar measurement on 26 May 1999, shown in Fig. 8c.; a pronounced Asian influence is demonstrated for altitudes above 5 km.

ACPD
10, 30473–30537, 2010

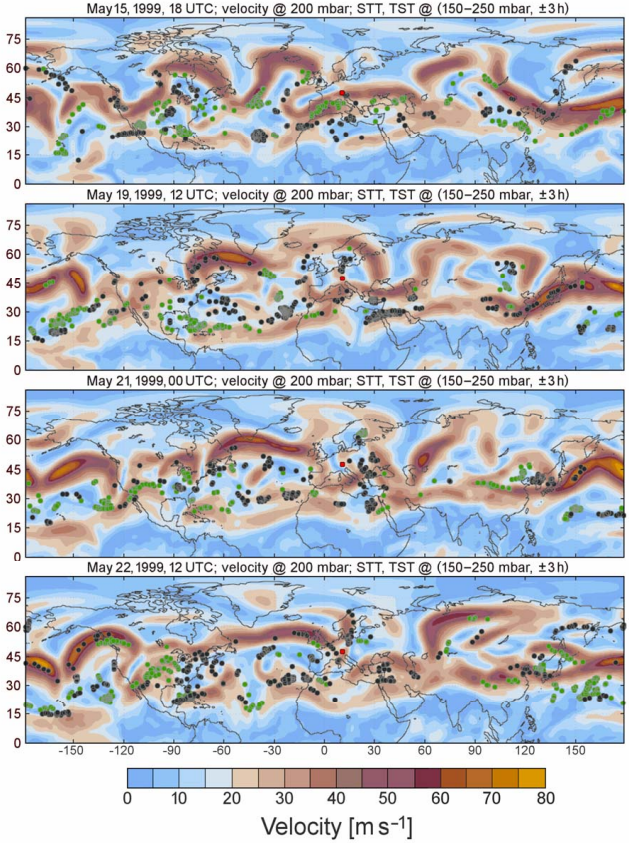

Fig. 14. Selected examples of the LAGRANTO visualizations of the jet streams for Case 2; the position of Garmisch-Partenkirchen is marked with a red dot next to the centre of each panel. The positions where trajectories revealed STT or TST between 150 and 200 mbar are marked by green and black dots, respectively.

ACPD
10, 30473–30537, 2010

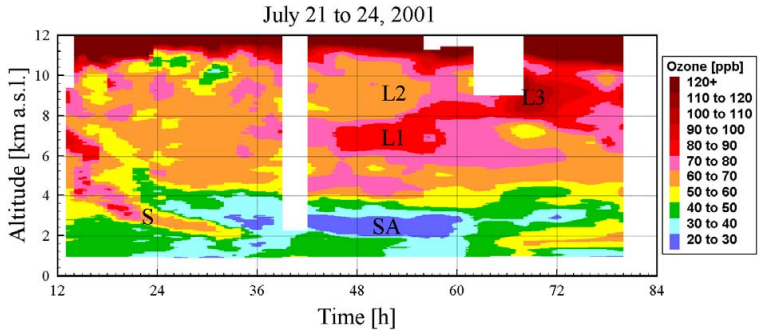

Fig. 15. Ozone sounding series in July 2001 at the beginning of a high-pressure period; S marks a stratospheric air intrusion, SA air from subtropical Atlantic, the layers marked with the labels L1, L2 and L3 are discussed in the text. The time scale is given with respect to 00:00 CET on 21 July.

ACPD
10, 30473–30537, 2010

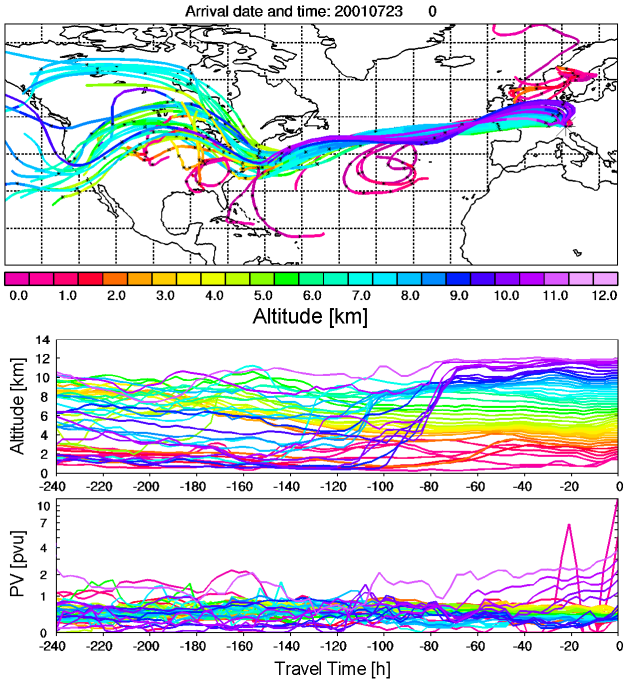

Fig. 16. Ten-day FLEXTRA backward trajectories initiated above Garmisch-Partenkirchen on 23 July 2001, 01:00 CET (corresponding to labels 1 and 2 in Fig. 15); the colour code in the upper panel describes the altitude at a given time. In the lower two panels it indicates the altitude at the location of Garmisch-Partenkirchen (t=0). The asterisks on the individual trajectories mark the 00:00 UTC positions.

ACPD
10, 30473–30537, 2010

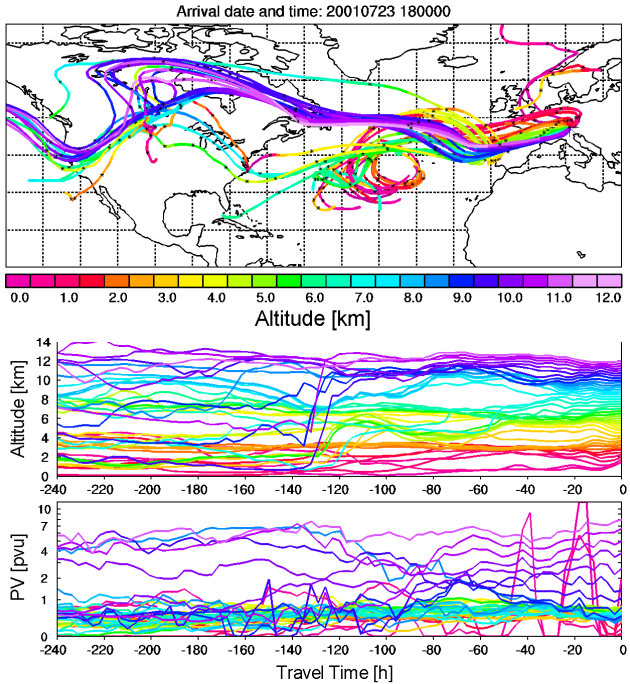

Fig. 17. Same as Fig. 16, but for 23 July 2001, 19:00 CET (corresponding to label 3 in Fig. 14); some of the upper-tropospheric trajectories reach altitudes above 12 km during the earliest period.

ACPD
10, 30473–30537, 2010

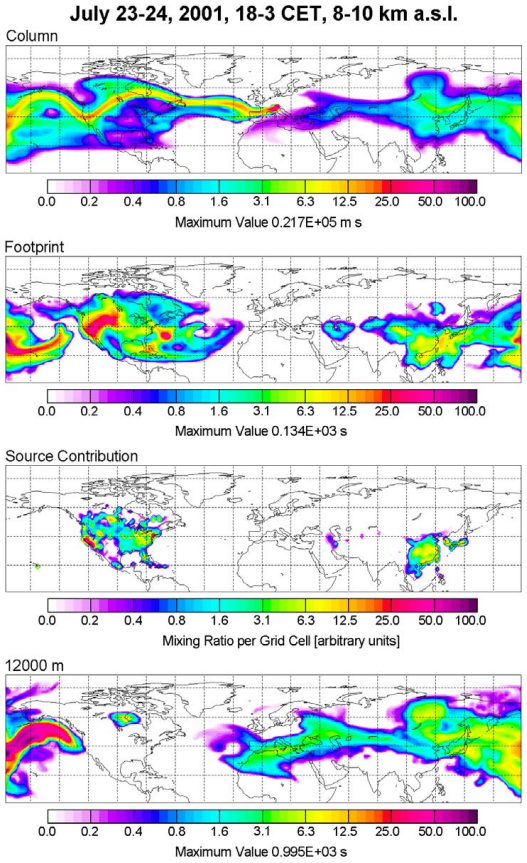

Fig. 18. FLEXPART fifteen-day backward simulation for retroplumes released between 23 July 2001, 18:00 CET, to 24 July 2001, 03:00 CET, and between 8 and 10 km a.s.l. above Garmisch-Partenkirchen (layer L3 in Fig. 15).

ACPD
10, 30473–30537, 2010

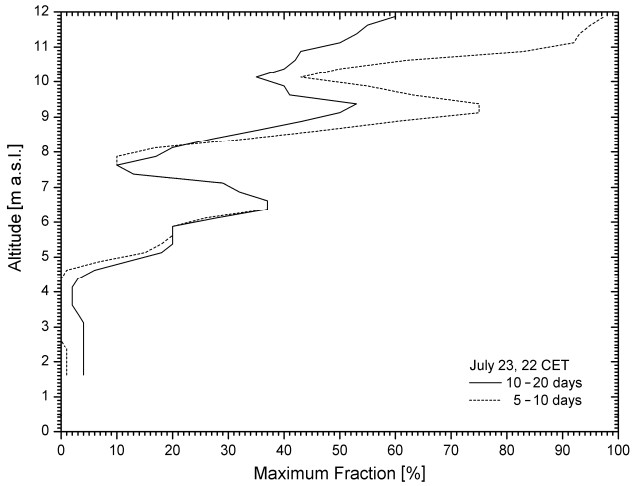

Fig. 19. Vertical distribution of the maximum stratospheric fraction in the retroplume calculated for 23 July, 22:00 CET, for two different backward time periods.

ACPD
10, 30473–30537, 2010

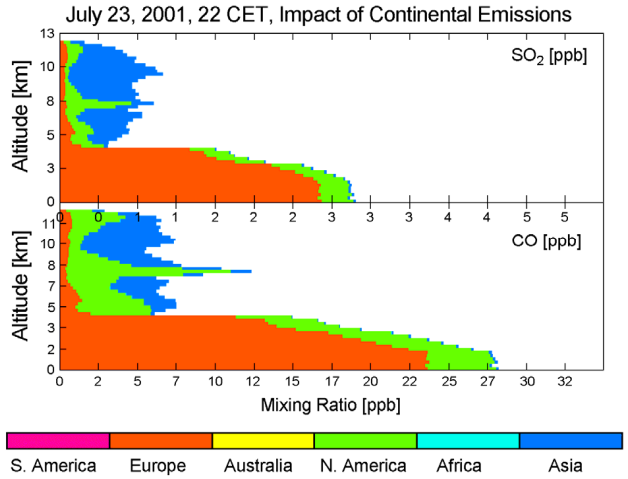

Fig. 20. Vertical distribution of SO_2 and CO emission tracers from the different source continents simulated for the lidar measurement on 23 July 1999, 22:00 CET.

ACPD
10, 30473–30537, 2010

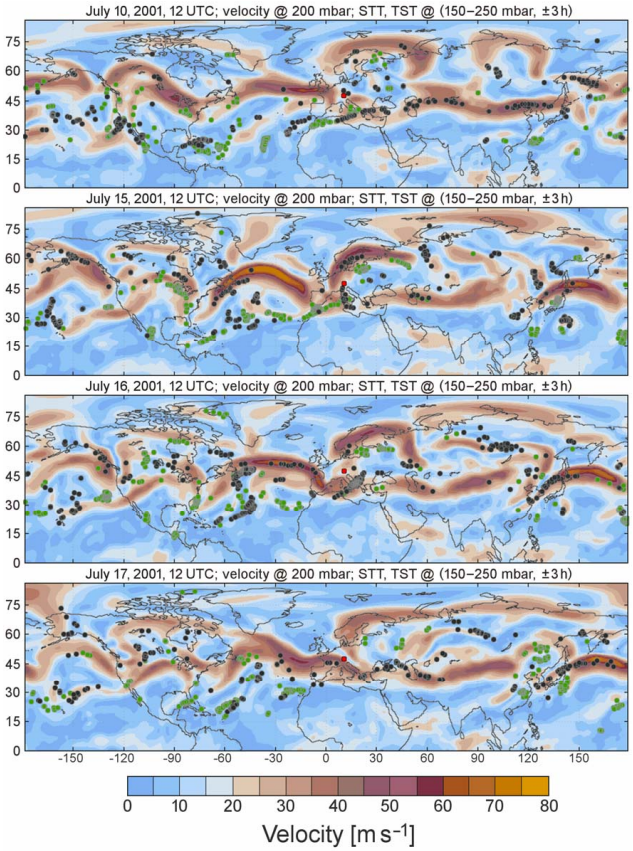

Fig. 21. Selected examples of the LAGRANTO visualizations of the jet streams for Case 5; the position of Garmisch-Partenkirchen is marked with a red dot next to the centre of each panel. The positions where trajectories revealed STT or TST between 150 and 200 mbar are marked by green and black dots, respectively.

ACPD
10, 30473–30537, 2010